NATIONAL HURRICANE RESEARCH PROJECT

REPORT NO. 40

On Initiation of Tropical Depressions and Convection in a Conditionally Unstable Atmosphere

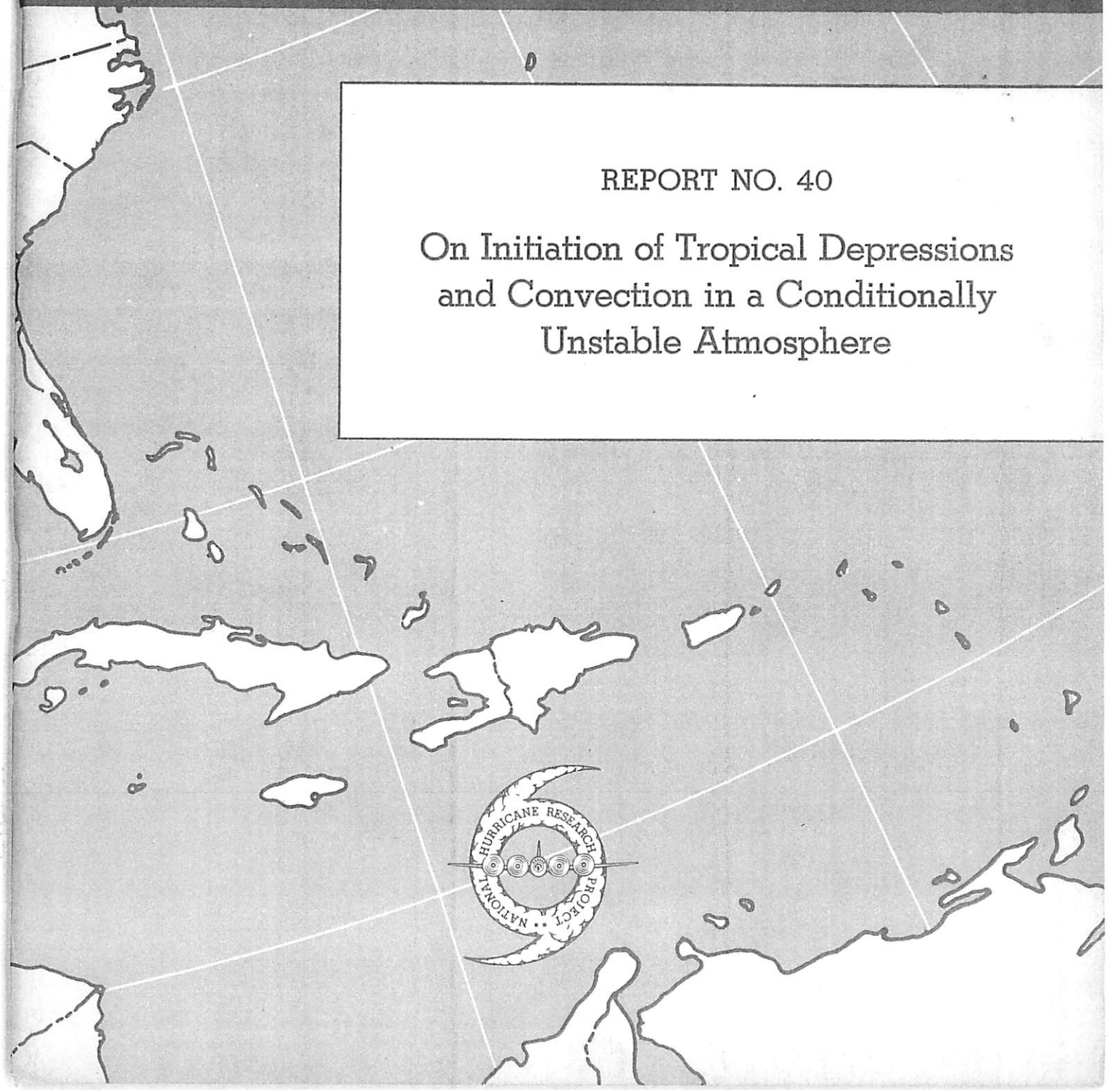

U. S. DEPARTMENT OF COMMERCE
Frederick H. Mueller, Secretary
WEATHER BUREAU
F. W. Reichelderfer, Chief

NATIONAL HURRICANE RESEARCH PROJECT

REPORT NO. 40

On Initiation of Tropical Depressions and Convection in a Conditionally Unstable Atmosphere

by

H. L. Kuo

Department of Meteorology, Massachusetts Institute of Technology

Final Report on contract Cwb-9488 and Cwb-9726

Washington, D. C.
October 1960

NATIONAL HURRICANE RESEARCH PROJECT REPORTS

Reports by Weather Bureau units, contractors, and cooperators working on the hurricane problem are pre-printed in this series to facilitate immediate distribution of the information among the workers and other interested units. As this limited reproduction and distribution in this form do not constitute formal scientific publication, reference to a paper in the series should identify it as a pre-printed report.

No. 1. Objectives and basic design of the NHRP. March 1956.
No. 2. Numerical weather prediction of hurricane motion. July 1956.
Supplement: Error analysis of prognostic 500-mb. maps made for numerical weather prediction of hurricane motion. March 1957.
No. 3. Rainfall associated with hurricanes. July 1956.
No. 4. Some problems involved in the study of storm surges. December 1956.
No. 5. Survey of meteorological factors pertinent to reduction of loss of life and property in hurricane situations. March 1957.
No. 6. A mean atmosphere for the West Indies area. May 1957.
No. 7. An index of tide gages and tide gage records for the Atlantic and Gulf coasts of the United States. May 1957.
No. 8. Part I. Hurricanes and the sea surface temperature field.
Part II. The exchange of energy between the sea and the atmosphere in relation to hurricane behavior. June 1957.
No. 9. Seasonal variations in the frequency of North Atlantic tropical cyclones related to the general circulation. July 1957.
No.10. Estimating central pressure of tropical cyclones from aircraft data. August 1957.
No.11. Instrumentation of National Hurricane Research Project aircraft. August 1957.
No.12. Studies of hurricane spiral bands as observed on radar. September 1957.
No.13. Mean soundings for the hurricane eye. September 1957.
No.14. On the maximum intensity of hurricanes. December 1957.
No.15. The three-dimensional wind structure around a tropical cyclone. January 1958.
No.16. Modification of hurricanes through cloud seeding. May 1958.
No.17. Analysis of tropical storm Frieda, 1957. A preliminary report. June 1958.
No.18. The use of mean layer winds as a hurricane steering mechanism. June 1958.
No.19. Further examination of the balance of angular momentum in the mature hurricane. July 1958.
No.20. On the energetics of the mature hurricane and other rotating wind systems. July 1958.
No.21. Formation of tropical storms related to anomalies of the long-period mean circulation. September 1958.
No.22. On production of kinetic energy from condensation heating. October 1958.
No.23. Hurricane Audrey storm tide. October 1958.
No.24. Details of circulation in the high energy core of hurricane Carrie. November 1958.
No.25. Distribution of surface friction in hurricanes. November 1958.
No.26. A note on the origin of hurricane radar spiral bands and the echoes which form them. February 1959.
No.27. Proceedings of the Board of Review and Conference on Research Progress. March 1959.
No.28. A model hurricane plan for a coastal community. March 1959.
No.29. Exchange of heat, moisture, and momentum between hurricane Ella (1958) and its environment. April 1959.
No.30. Mean soundings for the Gulf of Mexico area. April 1959.
No.31. On the dynamics and energy transformations in steady-state hurricanes. August 1959.
No.32. An interim hurricane storm surge forecasting guide. August 1959.
No.33. Meteorological considerations pertinent to standard project hurricane, Atlantic and Gulf Coasts of the United States. November 1959.
No.34. Filling and intensity changes in hurricanes over land. November 1959.
No.35. Wind and pressure fields in the stratosphere over the West Indies region in August 1958. December 1959.
No.36. Climatological aspects of intensity of typhoons. February 1960.
No.37. Unrest in the upper stratosphere over the Caribbean Sea during January 1960. April 1960.
No.38. On quantitative precipitation forecasting. August 1960.
No.39. On initiation of tropical depressions and convection in a conditionally unstable atmosphere. October 1960.

USCOMM-WB-DC

CONTENTS

	Page
Abstract	1
1. Introduction	2
2. Perturbation Equations	3
3. The Boundary Conditions	10
4. The Growth Rate and Most Preferred Scale	12
5. Most Preferred Scale and Marginal Stability	17
6. Convection in Saturated Conditionally Unstable Air	21
A. Nonviscous solution	22
B. Viscous solution and stability criterion	24
7. Solutions for Vertically Variable S	28
8. Vertical Transport of Heat and Modification of Mean Temperature Distribution by Convection	35
9. Composite Variation	41
10. Disturbances in Unsaturated Atmosphere and Initiation of Large-Scale Circulation	42
11. Conclusions	44
References	46

ON INITIATION OF TROPICAL DEPRESSIONS AND CONVECTION IN A CONDITIONALLY UNSTABLE ATMOSPHERE

H. L. Kuo

[Manuscript received April 25, 1960; revised August 8, 1960]

ABSTRACT

The analysis shows that if the stratification is unstable for ascending motion over an infinite area and small random perturbations of various scales are introduced, the final disturbance evolved will have the dimension of a cumulus cloud. The stable stratification in the descending region has the effect of increasing the critical lapse rate and making it independent of the actual values of viscosity and conductivity. It also tends to narrow the ascending region and to make the descending motion widespread, but its effect on the most favored scale of the ascending motion is insignificant. Even though a large horizontal eddy viscosity favors the large-scale motion, its introduction seems not entirely justifiable.

On the other hand, if the conditionally unstable atmosphere is originally unsaturated, and if saturation is produced only in a limited region, by the perturbation, it is then necessary to have the vertical velocity of the perturbation above a certain threshold value. Under this circumstance, the disturbances may organize themselves into a large-scale circulation.

The effects of stable layers above and below the unstable layer have been investigated by the use of three models, two based on a constant static stability factor in each layer and the third model with stability factor increasing with height. The results from all these models show a rapid decrease of the perturbation in the stable layer, but the temperature field obtained from the first two models is discontinuous while that derived from the third model is continuous. It has also been shown that the effect of the convective transport of heat is to make the middle troposphere nearly adiabatic (moist) and the upper part more stable.

The maximum vertical velocity that can be derived from the unstable tropical atmosphere is about 15 m. sec.$^{-1}$ if the convection is of the cumulus cloud type, and the corresponding horizontal velocity is about 30 m. sec.$^{-1}$. If the motion developed is of much larger horizontal dimension, the velocity will be mainly horizontal.

1. INTRODUCTION

Unless specific initial conditions that lead to the formation of the tropical storms have been found, we can only interpret their initiation in terms of the growth of small perturbations due to some kind of instability. It is generally accepted that the main source of energy of the tropical storms is the latent heat of condensation, and that horizontal temperature contrast is almost absent during the initial stage of their development. On the basis of these facts, it would seem appropriate to attribute the initiation of these storms to the unstable stratification of the atmosphere, expressed in terms of the equivalent potential temperature θ_e, which includes the effect of the water vapor content. Such an instability theory of origin of the tropical storms has been proposed by many theoretical meteorologists, for example, Haque [6], Syōno [12], and most recently Lilly [10].

In these theories, the authors attributed the formation of the tropical storms directly to the unstable stratification by identifying the storms with the limiting perturbation whose growth rate is zero, while disregarding all the other growing disturbances. However, since in the linear stability theory one assumes that small perturbations of all scales are present, the final motion that evolves from the system must be dominated by the perturbation with the highest growth rate, or the one which starts at the lowest Rayleigh number, unless some other physical processes are present which prevent the continued growth of this component. Therefore on the basis of the linear theory, one can only expect the motion field to be dominated by the component with the largest growth rate.

In this paper we shall at first study the nature of the small perturbations in an absolutely unstable or a conditionally unstable atmosphere, and then determine the most preferred scale of motion by finding the one which yields the highest growth rate. The effects of the hydrostatic and the balance approximations on the solutions will also be analyzed. It will be shown that in such an atmosphere which is at rest and is either absolutely or conditionally unstable, only cumulus cloud type convection can be expected to evolve if random infinitesimal perturbations are introduced. An organizing mechanism is definitely needed in order to build up a large-scale circulation if unstable stratification is the source of energy.

The second aim of this paper is to explore the possible mechanism which will produce such an organizing effect. It will be shown that such an organizing effect can be produced in an unsaturated conditionally unstable atmosphere by random but finite perturbations if the vertical velocity associated with the longer waves exceeds a threshold velocity of about 2 cm. sec.$^{-1}$.

Thirdly, the effect of stable layers above and below the unstable layer on convection will be investigated. We shall also determine the maximum vertical and horizontal velocities attainable from the unstable stratifications observed in the Tropics, and obtain the vertical transport of heat and the mean temperature distribution from the solution.

2. PERTURBATION EQUATIONS

In order to investigate the stability of the fluid due to vertical variation of temperature, we divide the temperature T, the pressure p and the density ρ into two parts: an equilibrium part and a departure from this equilibrium, represented by T_o, p_o, ρ_o, and T', p', ρ'. We assume that the equilibrium state is a state of no motion, therefore the quantities T_o, p_o, and ρ_o are functions of the vertical coordinate z only. Further p_o and ρ_o are related by the hydrostatic equation

$$\frac{\partial p_o}{\partial z} = - g\rho_o \tag{2.1}$$

where g is the gravity acceleration. In addition, the equation of state gives

$$p_o = R\,\rho_o T_o \tag{2.2}$$

where R is the universal gas constant.

Since T_o is the equilibrium temperature when the fluid is at rest, its vertical distribution is determined by the nonadiabatic processes such as heat conduction, radiation, and condensation and evaporation. Heat conduction alone will give a linear dependence on z, while the other nonadiabatic processes may result in more complicated vertical variations. Here we merely consider T_o as a known function of z.

In dealing with a gas medium it is more convenient to use the potential temperature θ, defined by the relation

$$\theta = T \left(\frac{P}{p} \right)^{\kappa} \tag{2.3}$$

where P is a standard pressure, usually taken as 1000 mb., and $\kappa = R/c_p$, c_p being the specific heat under constant pressure. We also divide θ into an equilibrium part θ_o, and a departure θ'.

Since the departures p', T', ρ', and θ' are usually much smaller than the corresponding equilibrium

$$\begin{aligned} \frac{\rho'}{\rho_o} &= \frac{p'}{p_o} - \frac{T'}{T_o} \\ &= \frac{p'}{\gamma_o} - \frac{\theta'}{\theta_o} \end{aligned} \tag{2.4}$$

where $\gamma = c_p / c_v$.

In what follows, we shall make use or the following symbols:

u, v = components of the horizontal velocity vector $\vec{v}_h$.

w = vertical velocity.

k = vertical wave number.

$\nabla_h = \vec{i}\,\frac{\partial}{\partial x} + \vec{j}\,\frac{\partial}{\partial y}$ is the horizontal delta operator.

$\nabla^2 = \nabla_h^2 + \frac{\partial^2}{\partial z^2}$, ∇_h^2 = two-dimensional Laplacian operator.

$$\mathcal{L} = \frac{\partial}{\partial t} - \nu_h \nabla_h^2 - \nu_z \frac{\partial^2}{\partial z^2}, \quad \mathcal{L}' = \frac{\partial}{\partial t} - K_h \nabla_h^2 - K_z \frac{\partial^2}{\partial z^2}, \quad \mathcal{L}_1 = \mathcal{L}_2 = \mathcal{L}.$$

ν_h, ν_z = horizontal and vertical kinematic viscosity, or their equivalences.

K_h, K_z = horizontal and vertical thermometric conductivity, or their equivalences. Part of the radiation process is approximated by a conductive process.

$c_o = \sqrt{\gamma R T_o}$, velocity of sound.

f = Coriolis parameter.

Q = rate of addition of heat to unit mass by nonadiabatic processes other than heat conduction.

Neglecting perturbation quantities of higher order, we have the following equations of motion, first law of thermodynamics, and continuity equation:

$$\mathcal{L} u - fv = -\frac{1}{\rho_o}\frac{\partial p'}{\partial x} \tag{2.5}$$

$$\mathcal{L} v + fu = -\frac{1}{\rho_o}\frac{\partial p'}{\partial y} \tag{2.6}$$

$$\mathcal{L}_1 w = -\frac{1}{\rho_o}\left(\frac{\partial p'}{\partial z} + \frac{g}{c_o^2} p'\right) + \frac{g\theta'}{\theta_o} \tag{2.7}$$

$$\mathcal{L}' \theta' + w \frac{\partial \theta_o}{\partial z} = \frac{Q}{c_p} \tag{2.8}$$

A different symbol $\mathcal{L}_1$ has been used for the operator $\mathcal{L}$ in the vertical equation of motion in order to see more clearly the effects of the departure from the hydrostatic approximation.

It can easily be shown that the local change of density in the continuity equation is important only for the high frequency gravitational and sound waves whose period is less than 3 minutes. Excluding these high frequency waves from the present investigation we may write the continuity equation as

$$\nabla_h \cdot \vec{v}_h + \frac{1}{\rho_o} \frac{\partial(\rho_o w)}{\partial z} = 0 \tag{2.9}$$

The vertical distribution of the undisturbed mean density ρ_o is related to the mean temperature distribution by the following relation

$$\sigma = \frac{g}{c_o^2} + s \tag{2.10}$$

where $\sigma \equiv - \partial \log \rho_o / \partial z$, $s = \partial \log \theta_o / \partial z$. In the earth's atmosphere, the value of s is about 1.0×10^{-5} m.$^{-1}$ while the values of σ and g/c_o^2 are about 1.0×10^{-4} m.$^{-1}$. We may therefore replace g/c_o^2 in equation (2.7) by σ *, and obtain the following approximation

$$\mathcal{L}_1 w = - \frac{1}{\rho_o} \left(\frac{\partial p'}{\partial z} + \sigma p' \right) + \frac{g\theta'}{\theta_o} . \tag{2.7a}$$

Eliminating θ' between (2.7a) and (2.8), disregarding the variation of ρ_o in applying the operator $\mathcal{L}$, we obtain

$$(gs + \mathcal{L}_1 \mathcal{L}') (\rho_o w) = - \mathcal{L}' \left(\frac{\partial p'}{\partial z} + \sigma p' \right) + \frac{g\rho_o}{c_p \theta_o} Q. \tag{2.11}$$

---

*When the local change of density is taken into consideration in the continuity equation, s will be added to g/c_o^2 so that we shall have σ instead of g/c_o^2 in the final equation for w.

Applying the operators $\nabla_h \times$ and $\nabla_h \cdot$ to the vectorial horizontal equation of motion and then solving for the vorticity $\zeta \equiv \nabla_h \times \vec{v}_h$ and the divergence $\nabla_h \cdot \vec{v}_h$ from the two resulting equations, we obtain

$$(f^2 + \mathcal{L}^2)\, \zeta = \frac{f}{\rho_o} \nabla_h^2 p' \tag{2.12}$$

$$(f^2 + \mathcal{L}^2)\, \nabla_h \cdot \vec{v}_h = - \frac{\mathcal{L}}{\rho_o} \nabla_h^2 p' \tag{2.13}$$

where ∇_h^2 is the horizontal Laplacian operator.

Now if we treat $\mathcal{L}$ as a factor rather than an operator, we may take the ratio of these two equations and find

$$\frac{\nabla_h \cdot \vec{v}_h}{\zeta} = - \frac{\mathcal{L}}{f} . \tag{2.14}$$

which shows that in a rotating system with small friction and slow time variation, the horizontal divergence is always small compared with the vertical component ζ of the vorticity. In other words, the motion should be mainly geostrophic for such motions.

This fact leads to another mathematical simplification which is often used in meteorology, that is, the quasi-geostrophic or balance condition. This approximation is equivalent to the neglecting of $\mathcal{L}^2$ against f^2 in (2.12) and (2.13). When the variables are independent of y, this approximation is the same as neglecting $\mathcal{L}u$ in (2.5). To analyze the effect of this approximation, let us use $\mathcal{L}_2$ instead of $\mathcal{L}$ in the first equation of motion so that we may have

$$\mathcal{L}_2 u - fv = - \frac{1}{\rho_o} \frac{\partial p'}{\partial x}. \tag{2.5a}$$

$$(f^2 + \mathcal{L}\mathcal{L}_2)\, \nabla_h \cdot \vec{v}_h = - \frac{\mathcal{L}}{\rho_o} \nabla_h^2 p'. \tag{2.15}$$

Eliminating $\nabla_h \cdot \vec{v}_h$ between (2.9) and (2.15) we obtain

$$(f^2 + \mathcal{L}\mathcal{L}_2) \frac{\partial}{\partial z} (\rho_o w) = \mathcal{L} \nabla_h^2 p'. \tag{2.16}$$

Finally, eliminating p' between the equations (2.11) and (2.16) and introducing the new dependent variable ω defined by

$$\omega = \rho_o e^{\sigma z/2} w \tag{2.17}$$

we obtain the following equation in ω:

$$\mathcal{L}' (f^2 + \mathcal{L}\mathcal{L}_2) \left(\frac{\partial^2 \omega}{\partial z^2} - \frac{\sigma^2}{4} \omega \right) + \mathcal{L}(gs + \mathcal{L}_1 \mathcal{L}') \nabla_h^2 \omega = \frac{g\rho_o e^{\sigma z/2}}{c_p \theta_o} \mathcal{L} \nabla_h^2 Q. \tag{2.18}$$

When f is zero, a factor $\mathcal{L}$ can be removed from this equation.

In this study we shall be concerned only with the nonadiabatic addition of heat Q due to condensation, which is considered to be determined by vertical motion alone. Thus we shall assume

$$\left.\begin{aligned} Q &= - L \frac{dm}{dt} = - L w \frac{\partial m}{\partial z} \quad \text{for saturated upward motion,} \\ Q &= 0 \qquad\qquad \text{for unsaturated or descending motion.} \end{aligned}\right\} \tag{2.19}$$

Here m is the mixing ratio of the air and L is the latent heat of condensation. With this Q we may combine the term on the right hand side of equation (2.18) with the last term on the left by introducing the stability factor S, defined by

$$\begin{aligned} S &= - s - \frac{L}{c_p \theta} \frac{\partial m}{\partial z} = - \frac{1}{\theta} \frac{\partial \theta_E}{\partial z} \quad \text{for saturated ascending motion} \\ &= \frac{T}{\theta} (\beta - \Gamma') = S_E \\ S &= - s = \frac{T}{\theta} (\beta - \Gamma) \quad \text{for unsaturated or descending motion.} \end{aligned} \tag{2.20}$$

In this form S is always discontinuous across the plane separating the ascending and descending motions.

The mean vertical distributions of the factors s and S_E in the Tropics are plotted in figure 1. These values are deduced from the mean soundings over West Indies published recently by Jordan [8,9]. The data show that during the hurricane season (July-Oct.) the stratification is more unstable (conditional) than the annual mean throughout the troposphere.

Since the operator $\mathcal{L}$ involves $\nu \nabla^2$ while $\mathcal{L}'$ involves $K \nabla^2$, equation (2.18) is of eighth order in z. However, for some special problems the order of the equation can be lowered. For example, for steady state solutions we have $\mathcal{L} = \frac{\nu}{K} \mathcal{L}'$, while for inviscid flow we have $\mathcal{L} = \mathcal{L}'$ $\left(= \frac{\partial}{\partial t} \right)$. This is

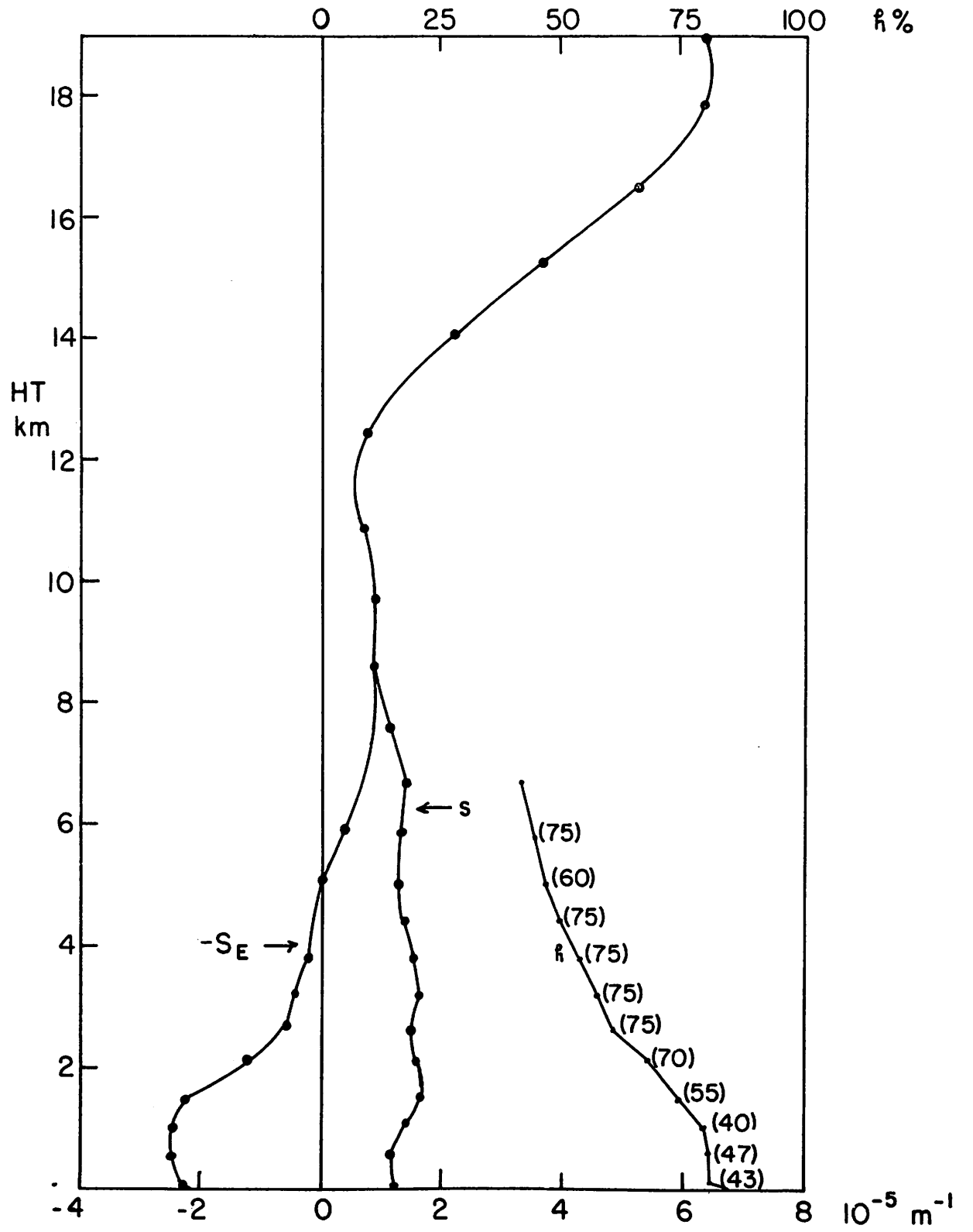

Figure 1. - Vertical distributions of the stability factors S and the relative humidity h in West Indies during the hurricane season (July-October). The numbers in the parentheses along the h-curve indicate the lift (in mb.) needed to produce saturation.

also the case if $\nu = K$. Since for application to many atmospheric problems we must use eddy viscosity and eddy conductivity whose values are rather uncertain, we may put $\mathcal{L} = \frac{\nu}{K}\mathcal{L}'$ and remove one factor from the equation by replacing g by $\frac{\nu}{K} g \equiv g'$. Equation (2.18) then reduces to the following

$$(f^2 + \mathcal{L}\mathcal{L}_2)\left(\frac{\partial^2\omega}{\partial z^2} - \frac{\sigma^2}{4}\omega\right) - (g'S - \mathcal{L}\mathcal{L}_1)\nabla_h^2\omega = 0. \qquad (2.21)$$

This equation shows that in discussing the stability problem for motions produced by unstable stratification one cannot make use of the hydrostatic approximation ($\mathcal{L}_1 = 0$) and the balance approximation ($\mathcal{L}_2 = 0$) at the same time, because if one does, the differential equation will contain no $\mathcal{L}$ operator and the prospect of instability is completely lost. What is left is the steady state non-viscous equation for the disturbance with the largest horizontal scale possible and it will then be impossible to draw any conclusion concerning the smaller disturbances. In this respect the stability problem for an unstable vertical stratification is quite different from that of horizontal baroclinicity, because for the latter problem the essential result can be obtained by assuming both hydrostatic and balance approximations.

To the present approximation, the effect of the departure from the hydrostatic equilibrium is represented by the last term alone. This term may be neglected for the disturbances whose horizontal scale is much larger than the vertical scale (i.e., for disturbances for which $\nabla_h^2 \ll \partial^2/\partial z^2$). Unless such restrictions are made, the hydrostatic approximation will lead to error. On the other hand, for problems of atmospheric motion the term containing the factor σ^2 is usually much smaller than the first term and can be neglected.

In discussing the explicit form of the horizontal variation of ω we shall make the additional simplifying assumption that the various quantities have circular symmetry, with a view to the application to convective circular vortices. Since the effect of local change of density has been neglected, we may introduce a Stokes stream function ψ, defined by

$$\rho_o r u = -\frac{\partial\psi}{\partial z}, \quad \rho_o r w = \frac{\partial\psi}{\partial r} \qquad (2.22a)$$

where u stands for the radial velocity. It is again more convenient to use the variable Ψ as the dependent variable, defined by

$$\Psi = \psi e^{\sigma z/2} \qquad (2.22b)$$

In terms of this variable, equation (2.21) becomes

$$(f^2 + \mathcal{L}\mathcal{L}_2)\left(\frac{\partial^2\Psi}{\partial z^2} - \frac{\sigma^2}{4}\Psi\right) - (g'S - \mathcal{L}\mathcal{L}_1)\nabla_h'^2\Psi = 0 \qquad (2.23)$$

where $\nabla_h'^2 = r \frac{\partial}{\partial r} \frac{1}{r} \frac{\partial}{\partial r}$. In the above equation, the operators $\mathcal{L}$, $\mathcal{L}_1$, and $\mathcal{L}_2$ all contain this horizontal Laplacian rather than ∇_h^2.

This equation will be solved by separation of variables through the substitution

$$\Psi = e^{qt} P(z) \phi (r) \tag{2.24}$$

Besides the case of a constant unstable stratification, we shall deal with the following types of S distributions:

A. Horizontal variations

(1) Constant unstable S (> 0) both for ascending and for descending motions

(2) Constant conditionally unstable stratification and saturated ascending air. S changes sign according to the sign of w.

B. Vertical distribution

(1) Constant unstable S (> 0) at all levels

(2) Constant unstable S in lower atmosphere and constant stable S (< 0) in upper atmosphere.

(3) S increases linearly with height, unstable below and stable above.

Because of the different S distributions we must use different solutions in different regions and join them across the internal boundaries. In order to simplify the solutions, we shall make the additional assumption that when S changes in the vertical direction it is constant horizontally, whereas when S varies horizontally it is constant along the vertical.

Thus either ϕ or P is a harmonic function. The case with S varying both vertically and horizontally will be discussed only briefly.

3. THE BOUNDARY CONDITIONS

The external boundaries of the system under consideration are horizontal planes at $z = 0$ and $z = \infty$. Since $\omega = \rho_o w e^{\sigma z/2}$ and $\rho_o = \rho_{oo} e^{-\sigma z}$ where ρ_{oo} is the mean sea level density, we must require the vanishing of ω both at the lower and at the upper boundary. The latter is necessary in order to have the kinetic energy per unit volume approach zero as z approaches infinity. Therefore two of the boundary conditions that must be satisfied by ω are

$$\omega = 0 \quad \text{at} \quad z = 0 \quad \text{and as} \quad z \to \infty . \tag{3.1}$$

When the viscous effect is taken into consideration in full, additional conditions must be imposed because the differential equation is of higher order. However, only in discussing the stability criterion and the preferred

scale of motion we will use equation (2.23) in its complete form, and there we will take S as a positive constant. In this case the vanishing of tangential stresses and of θ' shall be imposed. These conditions can be satisfied by harmonic solutions. In seeking solutions for a vertically variable stability factor, we shall approximate the viscous effect by replacing the Laplacian operator ∇^2 in the viscous term by a factor $-(k^2 + \alpha^2)$, which is equivalent to the use of a harmonic function as the solution in estimating the viscous effect.

In the horizontal directions the fluid is assumed to extend to infinity. The conditions we impose in the horizontal direction are either finiteness or periodicity of the solution. Specifically, for the case of circular symmetry we shall require the vanishing of the radial velocity u at the axis of symmetry. We shall also require u to vanish at $r = r_2$, which may be finite or infinite. In addition, $\frac{\partial w}{\partial r}$ is also assumed to vanish at these two radii. Thus the external boundary conditions in the r - direction are:

$$\phi = 0 \text{ and } \frac{d}{dr}\frac{1}{r}\frac{d\phi}{dr} = 0 \text{ at } r = 0 \text{ and } r = r_2. \tag{3.2}$$

It may be mentioned that for inviscid flow these two conditions are identical and therefore there is only one condition for each given value of r.

When the stability factor S varies discontinuously in space, we must impose certain conditions on the internal boundaries. Two necessary requirements are the continuity of the normal velocity v_n and of the pressure p'. In terms of the function Ψ, the first of these two conditions is equivalent to the continuity of Ψ, while the second depends upon the S variation.

A. S varies horizontally - conditional instability. When viscosity is neglected, the elimination of θ' between the equations (2.6a) and (2.7) gives

$$(g'S - q^2)\, w = \frac{q}{\rho_o}\left(\frac{\partial p'}{\partial z} + \sigma p'\right)$$

Since p' and $\frac{\partial p'}{\partial z}$ are continuous across the vertical boundary, the quantity on the left side of this equation must also be continuous. However, since S changes its sign and is discontinuous, w must also change its sign and have a finite discontinuity. Such a discontinuity has been revealed in the solution obtained by Haque [6].

In terms of the function ϕ, we have the following conditions across the vertical boundary for inviscid flow:

$$\phi_1 = \phi_2$$

$$\frac{d\phi_1}{dr} = -\ell'^2 \frac{d\phi_2}{dr}, \qquad \ell'^2 = \frac{-g'S_2 + q^2}{g'S_1 - q^2} \tag{3.3}$$

B. Vertically variable S. When viscosity is neglected, equations (2.5) and (2.6) show that the horizontal velocity components are continuous, implying the continuity of $\partial\Psi/\partial z$. Thus across a horizontal internal boundary we have

$$\text{(i)}\quad P_1 = P_2 \quad \text{and} \quad \text{(ii)}\quad \frac{dP_1}{dz} = \frac{dP_2}{dz}\,. \tag{3.4}$$

4. THE GROWTH RATE AND MOST PREFERRED SCALE

In an unstable layer with a constant stability factor $S = S_1 > 0$, the solution ω of equation (2.21) that satisfies the free boundary conditions is of the form

$$\omega = Ae^{qt} \sin k\zeta \quad F(x,y), \quad \zeta = \frac{\pi z}{h} \tag{4.1}$$

where $F(x,y)$ is a harmonic function satisfying the equation

$$\nabla_h^2 F = -\alpha^2 \frac{\pi^2}{h^2} F \tag{4.1a}$$

In dealing with atmospheric motions we should use the eddy coefficient of viscosity, which in general has different values in different directions. We shall denote the eddy viscosity coefficient in the horizontal directions by ν_h and that in the vertical direction by ν_z. When the solution (4.1) is substituted in equation (2.21), we find the relation

$$\gamma = \frac{g'S_1\alpha^2 - f^2(k^2 + \lambda^2)}{\alpha^2\gamma_1 + (k^2 + \lambda^2)\gamma_2}\,, \quad \lambda = \frac{\sigma h}{2\pi} \tag{4.2}$$

where γ is defined by

$$\gamma = q + \nu_z \frac{\pi^2}{h^2}(k^2 + \alpha'^2), \quad \alpha'^2 = \alpha^2 \nu_h/\nu_z\,. \tag{4.3}$$

and $\gamma_1 = \gamma_2 = \gamma$ when the equations (2.5) and (2.7) are taken in full. The length scale being used is a depth h, and α is the horizontal wave number and k is the vertical wave number.

Equation (4.2) shows that γ is either real or purely imaginary, according to whether $gS_1\alpha^2$ is greater or less than $f^2(k^2 + \lambda^2)$. In the latter case q will be complex but with a negative real-part. Therefore the solution represents the stable gravitational-internal wave with diminishing amplitude. It is also seen that the maximum value of q^2 corresponds to the first vertical mode of the solution, k = 1, if we take h as the effective depth. We shall use this value of k only.

The physical interpretation of this limiting wave number $\alpha_0^2 = f^2/gS$ is that for the perturbations with α smaller than α_0, the kinetic energy of the

horizontal motion generated by the Coriolis effect through a displacement is greater than the potential energy released, while the reverse is true for perturbations with α greater than α_o.

For earth's atmosphere, the value of λ^2 is about 0.025, which is much less than 1 and will be neglected in the following. Therefore the equation for q is given by

$$\gamma = \frac{gS\alpha^2 - f^2}{\alpha^2\gamma_1 + \gamma_2} \tag{4.2a}$$

In this section we shall examine the effects of various physical factors and different mathematical simplifications on the growth rate q and on the most preferred wave number α_m.

The values of q computed from equation (4.2a), with $\gamma_1 = \gamma_2 = \gamma$, $f = 5 \times 10^{-5}$ sec.$^{-1}$, h = 10 km. are plotted in figure 2 for three different values of S which often exist in the Tropics. The solid lines correspond to $\nu_h = \nu_z = 10^3$ m.^{2}sec.$^{-1}$, while the dashed curves correspond to inviscid motion. It is seen that when friction is neglected, q has its maximum when $\alpha = \infty$, whereas with friction the maximum q occurs at about $\alpha = \alpha_m \doteq 1.6$, with a very slow shift toward a lower value as S decreases.

Comparing the dashed curves with the corresponding full curves, we see that the effect of eddy viscosity on q is small for $\alpha < 1$. We also mention that except for very small values of α, the effect of the Coriolis parameter f is also small.

In computing the curves in figure 2, we have used $\nu_h = \nu_z$. The effect of the inhomogeneity of ν is included in (4.2) through the use of the quantity $\alpha'^2 = \alpha^2 \nu_h/\nu_z$. This equation and the curves in figure 2 show that the most preferred horizontal scale of the ascending motion will always be smaller than h if the ratio ν_h/ν_z is less than 1. On the other hand, when ν_h/ν_z is greater than 1, the preferred horizontal scale may become larger than h. For example, with all the other factors remaining the same, but with $\nu_h/\nu_z = 100$, then the most preferred horizontal scale of the ascending motion will be increased to about 6h.[1] Thus an effective way of increasing the preferred horizontal scale of motion in the present system is to increase the value of ν_h.

---

[1] For the case of line symmetry, the horizontal scale of the ascending motion is given by $x_1 = h/\alpha$. For circular symmetry, it is given by $r_1 = 2.405h/\pi\alpha$.

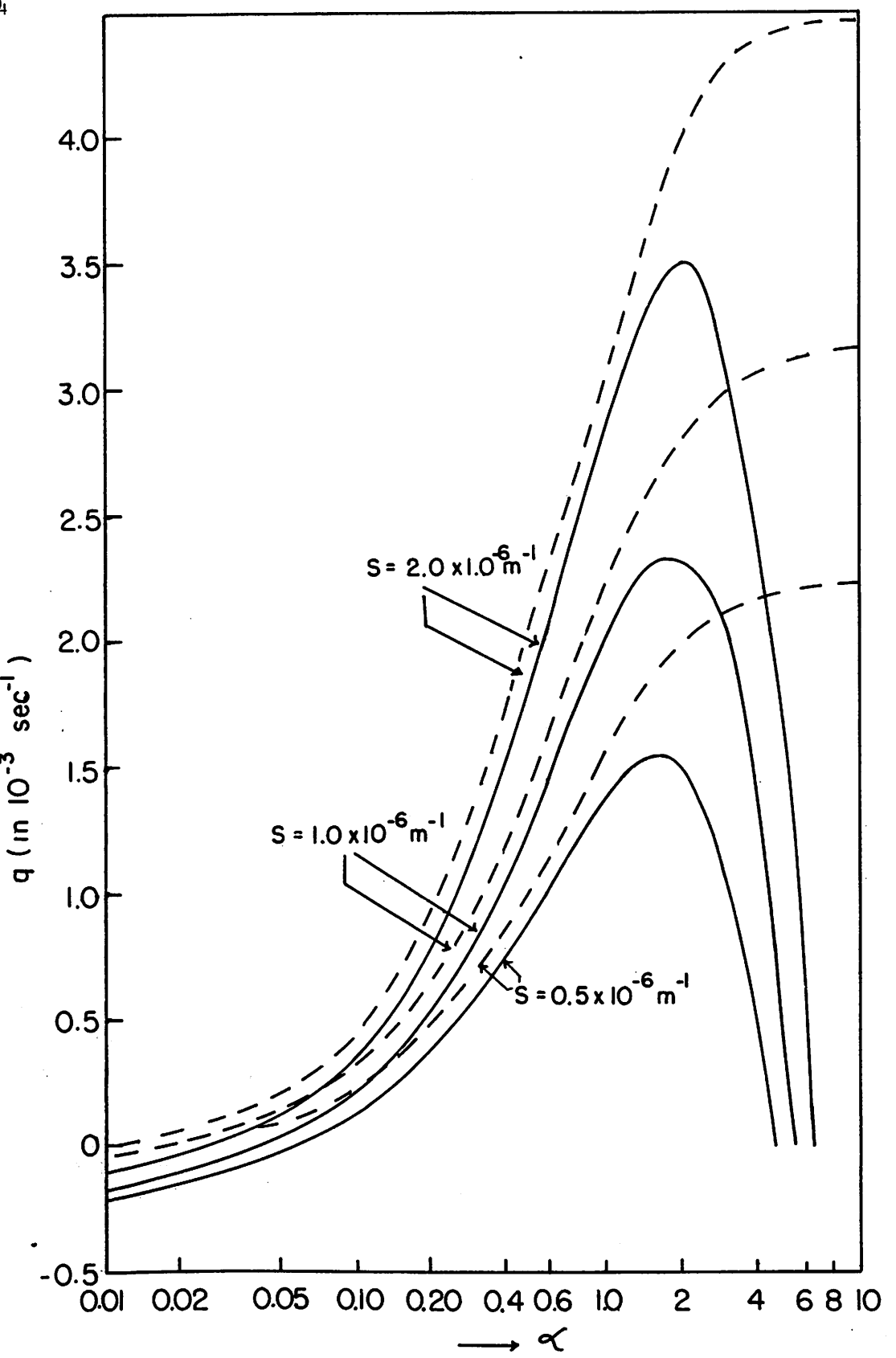

Figure 2. - The growth rate q as a function of the horizontal wave number for three different values of S. Dashed curves given by inviscid approximation, solid curves given by viscous equation for $\nu = 10^3 m.^2 sec.^{-1}$.

The effect of ground friction may be included by making use of the boundary condition

$$\frac{d\vec{V}_h}{dz} = C\vec{V}_h \tag{4.4}$$

at $z = \delta$, the height of the anemometer, instead of the condition (3.1). The result is to reduce the effective depth of the fluid. It may be remarked that since no basic flow is included in this model, ground friction cannot be expected to work as a driving force for the motion.

Returning to equation (4.2a) we see that both the hydrostatic ($\gamma_1 = 0$) and the balance ($\gamma_2 = 0$) approximations tend to overestimate the growth rate q, and when these two approximations are used simultaneously, they lead to an ($\pm$) infinite q for all disturbances whose horizontal dimensions are smaller (or larger) than the limiting scale given by $\alpha_o^2 = f^2/gS$, while for this limiting disturbance we have q = 0. Therefore these two approximations cannot be introduced simultaneously. On the other hand, one or part of these two approximations may be used without seriously damaging the system.

We shall now examine the effects of the following approximations on q:

$$\left.\begin{aligned}
&a_1:\ \gamma^2 = \frac{gS\alpha^2 - f^2}{1+\alpha^2},\ \mathcal{L}_1 = \mathcal{L}_2 = \mathcal{L};\ \text{full equations,}\\
&b_1:\ \gamma^2 = gS\alpha^2 - f^2,\ \mathcal{L}_1 = 0\ ;\ \text{hydrostatic,}\\
&c_1:\ \gamma^2 = gS - f^2/\alpha^2,\ \mathcal{L}_2 = 0\ ;\ \text{balance approximation}\\
&a_2:\ \gamma = \frac{gS\alpha^2 - f^2}{(1+\alpha^2)(1+\alpha'^2)A},\ \mathcal{L}_1 = \mathcal{L}_2 = A(1+\alpha'^2),\ A = \frac{\nu_z \pi^2}{h^2}.\\
&b_2:\ \gamma = \frac{gS\alpha^2 - f^2}{(1+\alpha'^2)A},\ \mathcal{L}_1 = 0,\ \mathcal{L}_2 = A(1+\alpha'^2);\ \text{hydrostatic}\\
&c_2:\ \gamma = \frac{gS\alpha^2 - f^2}{\alpha^2(1+\alpha'^2)A},\ \mathcal{L}_1 = A(1+\alpha'^2),\ \mathcal{L}_2 = 0;\ \text{balanced}
\end{aligned}\right\} \tag{4.5}$$

The values of q obtained from the equations ($4.5a_1$, b_1, c_1) have been plotted in figure 3a. The curves a_{11}, b_{11}, c_{11} are for $\nu_h/\nu_z = 1$, $S = 10^{-6}\,\text{m.}^{-1}$; and curves a_{12}, b_{12}, c_{12} are for $\nu_h/\nu_z = 10$, while the curves a_{13}, b_{13}, and c_{13} are for $\nu_h/\nu_z = 100$. The value of ν_z used is $10^3\,\text{m.}^2\text{sec.}^{-1}$ From these curves we see that both the hydrostatic and the balance approximations overestimate q, but the hydrostatic approximation is quite accurate for

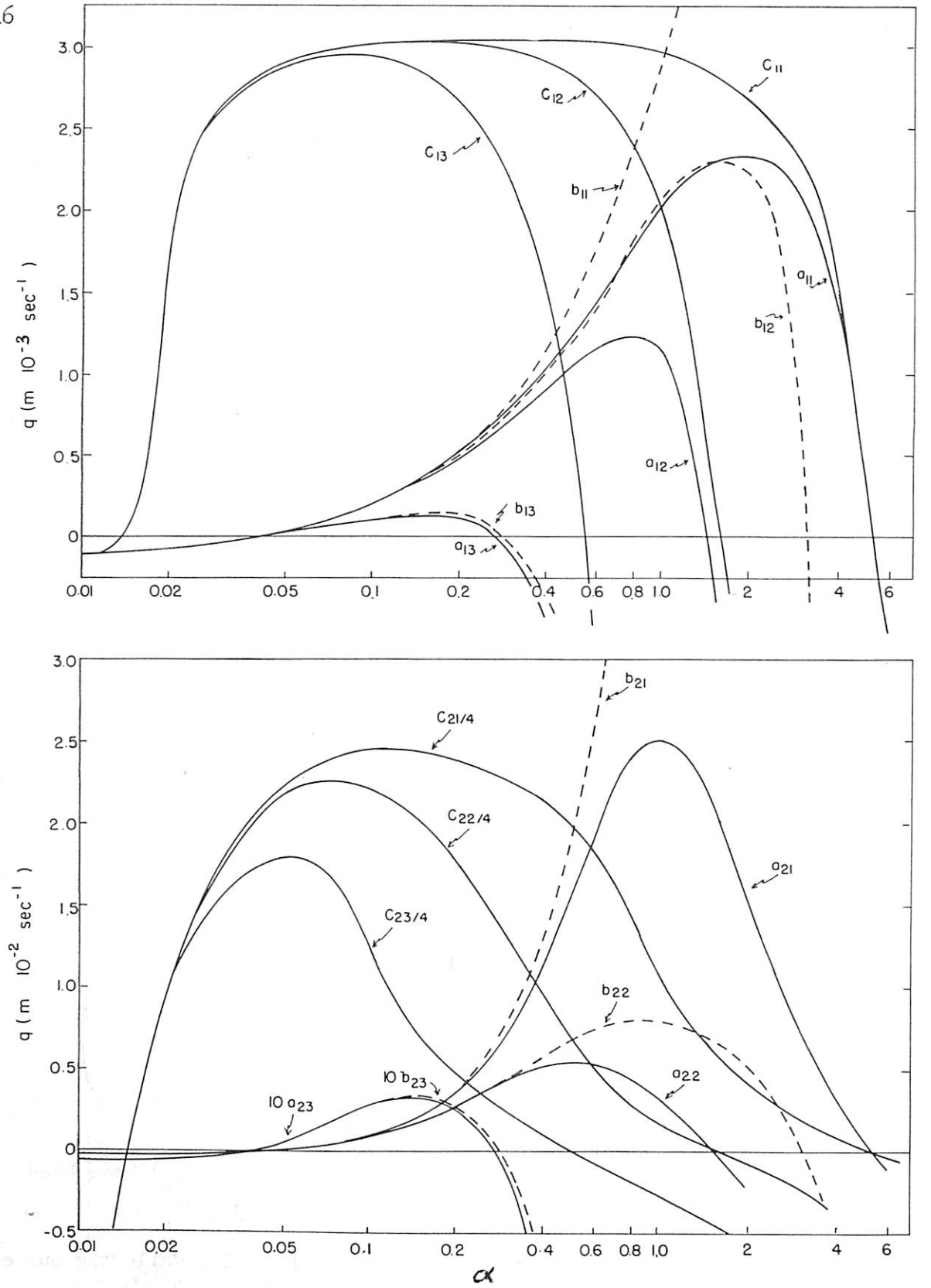

Figure 3. - Upper: Values of q as a function of α (the abscissa) for S = 10^{-6} m.$^{-1}$, as given by the equations ($4.5a_1$, b_1, c_1). Lower: Same as a, as given by the equations ($4.5a_2$, b_2, c_2).

the disturbances whose horizontal scale is larger than 6h ($\alpha < 0.16$). On the other hand, the balance condition seems to be a good approximation for the small scale disturbances. We also note the flatness of the c-curves.

If we neglect $\partial/\partial t$ but retain the viscous terms in the radial and vertical equations of motion, we then obtain equation ($4.5a_2$), while the equations b_2 and c_2 represent the corresponding hydrostatic and balance approximations. Here q occurs only in the first degree, therefore the motion is either amplified or damped but without oscillation. The values of q given by these equations are plotted in figure 3b for the same three values of ν_h/ν_z. It is seen that these q values are about 10 times larger than those in figure 3a; therefore, neglecting $\partial/\partial t$ in the radial and vertical equations of motion greatly exaggerates the growth and the damping rates. We also note the shift of the most preferred motion to a larger horizontal scale, which is particularly pronounced in the balance approximation ($4.5c_2$).

From the analysis above we see that neither the full perturbation equations nor the hydrostatic approximation show any preference to large-scale motion, but the complete balance requirement does produce a shift toward a larger horizontal scale. Thus, an efficient mathematical model which enhances the development of a large-scale convective system is obtained through the use of a large horizontal eddy viscosity coefficient and the requirement of a complete balance between the radial pressure gradient and the centrifugal force, but retaining the viscous terms in the vertical equation of motion.

However, it seems that neither the introduction of a very large ν_h nor the assumption of complete radial balance are fully justifiable from the present consideration; they can only be considered as mathematical devices to filter out the small-scale convections. Even though the presence of the cumulus cloud scale convection may have the effect of a large eddy viscosity for the large-scale convection, the arresting of the enormous growth of these small convections themselves must be due to some physical processes in these systems, such as the entrainment of dry air into the ascending current and the down draft and cooling produced by falling rain.

5. MOST PREFERRED SCALE AND MARGINAL STABILITY

The relation between S and α for marginal stability is obtained by letting q approach zero in (4.2). Introducing the nondimensional quantities R and T, defined by

$$R = \frac{g'Sh^4}{\nu^2\pi^4}, \quad T = \frac{f^2h^4}{\nu^2\pi^4}, \tag{5.1}$$

and setting $k = 1$, $\lambda = 0$, $\nu = \nu_h = \nu_z$, $\mathcal{L}_1 = b_1\mathcal{L}$, $\mathcal{L}_2 = b_2\mathcal{L}$, we then find

$$R = b_1(1+\alpha^2)^2 + \frac{1}{\alpha^2}[T + b_2(1+\alpha^2)^2], \tag{5.2}$$

when $b_1 = b_2 = 1$, this equation is identical to the equation obtained by Chandrasekhar [4].

For a given T, R, as given by equation (5.2), attains its minimum when α is given by

$$2 b_1 \alpha^4 (1 + \alpha^2) + b_2 (\alpha^4 - 1) = T. \tag{5.3}$$

The roots of this equation, which we designate by α_m, are given in table 1 for three different methods of computation. These in line a are from the full equation ($\mathcal{L}_1 = \mathcal{L}_2 = \mathcal{L}$), and those in line b are from the hydrostatic approximation ($\mathcal{L}_1 = 0, \mathcal{L}_2 = \mathcal{L}$), while those in line c are from the balance approximation ($\mathcal{L}_1 = \mathcal{L}, \mathcal{L}_2 = 0$). The corresponding values of the minimum R computed from (5.2) are also given in this table. Figure 4 illustrates the differences of these three computations. It is seen that the hydrostatic approximation tends to shift the most preferred motion to a still smaller horizontal scale, rather than giving a preference to large-scale motion. This is shown more clearly by the asymptotic expressions for large values of T. From either the full equation or the balance approximation we obtain

$$\begin{aligned} \alpha_m &\to \left(\frac{T}{2}\right)^{1/6} \\ R_m &\to 3 \left(\frac{T}{2}\right)^{2/3} \end{aligned} \qquad \text{as } T \to \infty. \tag{5.3a}$$

We note that for fixed ν, the critical temperature gradient S_c increases with $f^{4/3}$ while for fixed f, S_c is proportional to $\nu^{2/3}$ if we keep the Prandtl number constant. On the other hand, with the hydrostatic approximation we obtain

$$\begin{aligned} \alpha_m &\to T^{1/4} \\ R_m &\to 2T^{1/2} \end{aligned} \tag{5.3b}$$

Table 1. - Values of α_m and R_m for various values of T.

	T	0	1	10	100	1000	2500	5000
α_m	a	0.71	0.82	1.18	1.81	2.73	3.21	3.62
	b	1.05	1.19	1.82	3.17	5.62	7.01	8.41
	c		0.75	1.20	1.85	2.78	3.25	3.65
	R_m	6.75	8.44	17.02	54.39	214.67	382.8	596.7

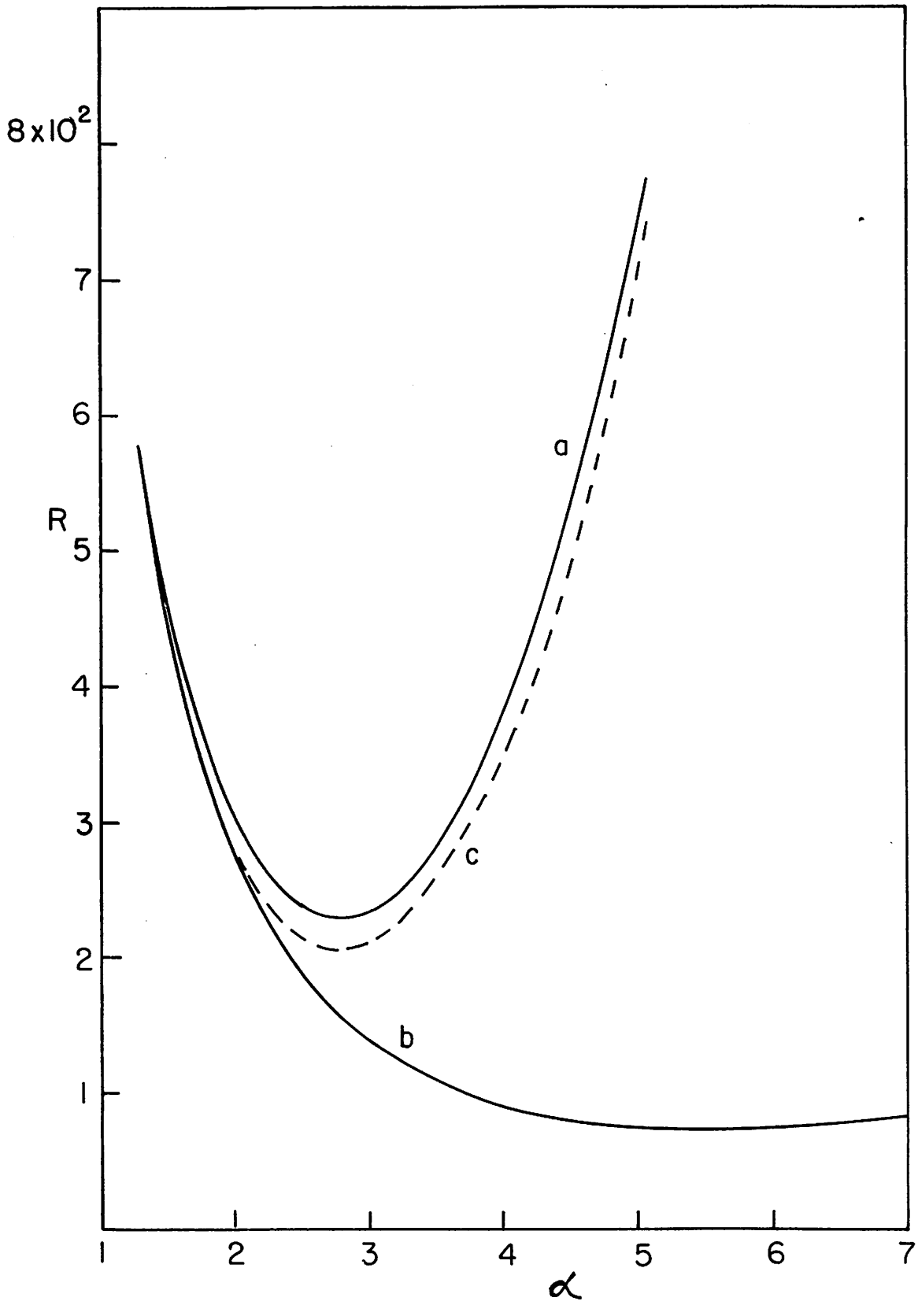

Figure 4. - The minimum critical Rayleigh number as a function of α for a Taylor number $T = 10^3$, obtained from the three different approximations.

We note that these critical values of R are many orders of magnitude smaller than the value of R given by the equivalent potential temperature in the Tropics. Under this circumstance, the motion is apt to be very turbulent.

The results obtained in these two sections show that the two selection rules are roughly equivalent to each other. This equivalence can be demonstrated more clearly by the application of the kinetic energy integral. Multiplying the nonlinearized equations of motion scalarly by $\vec{v}$, and making use of the continuity equation we obtain

$$\frac{\partial e}{\partial t} + \nabla \cdot \vec{v}(p + e) = \frac{g\rho_o}{\theta_o} w\theta' + sp'w + v_i \frac{\partial \tau_{ik}}{\partial x_k} \tag{5.4}$$

where $e = \frac{1}{2}\rho_o (u^2 + v^2 + w^2)$ is the kinetic energy per unit volume, and $\tau_{ik} = \mu_{(k)} \frac{\partial v_i}{\partial x_k}$ is the viscous stress, $\mu_{(k)}$ being the viscosity coefficient in the direction x_k. The summation convention over the repeated indices i and k has been used in the last term of this equation.

Integrating over the entire volume under consideration, assuming that the normal velocity vanishes on the boundary and neglecting the contribution from the second term on the right, which is usually much smaller than the first term, we then obtain

$$\frac{\partial K}{\partial t} = \frac{g}{V} \int \frac{\rho_o w \theta'}{\theta_o} dV - D \tag{5.4a}$$

where K is the average kinetic energy, $D = -\frac{1}{V}\int v_i \frac{\partial \tau_{ik}}{\partial x_k} dV$ is the average rate of dissipation, and the first integral on the right represents the conversion of potential energy into kinetic energy. It is evident that when the dissipation exceeds the rate of conversion, the kinetic energy decreases, whereas when the rate of conversion exceeds the dissipation, the kinetic energy increases.

In order to evaluate the various integrals, we make use of the solutions of the linearized equations, given by

$$\left.\begin{aligned} w &= Ae^{qt} \sin\frac{\pi z}{h} F'(x) \frac{h}{\pi} \\ u &= -Ae^{qt} \cos\frac{\pi z}{h} F(x) \\ v &= -(T^{1/2}/\overline{\gamma_1})\, u \\ \theta' &= -(1/\overline{\gamma_1}\,\kappa)(\partial\theta_o/\partial z)(h^2/\pi^2)\, w \end{aligned}\right\} \tag{5.5}$$

where $\overline{\gamma}_1 = 1 + \alpha^2 + q'$ and $\overline{\gamma}_1' = 1 + \alpha^2 + q' \frac{\kappa}{\nu}$, $q' = q \frac{h^2}{\nu \pi^2}$.

Substituting these solutions into (5.4a) we obtain

$$q' \left(\overline{\gamma}_1' + \frac{\kappa}{\nu}\right) \frac{\left(1 + \alpha^2 + \frac{T}{\overline{\gamma}_1^2}\right)}{\alpha^2} = R - \frac{(\alpha^2 + 1)^2}{\alpha^2} \left[1 + \alpha^2 + \frac{T}{\overline{\gamma}_1^2}\right] \quad (5.6a)$$

$$\equiv R - R_o$$

It is seen that the rate of conversion of potential energy into kinetic energy is represented by the Rayleigh number R, while the dissipation is represented by the last term of this equation, which we shall denote by R_o and call the "critical Rayleigh number." Thus only when the actual Rayleigh number R is greater than the critical Rayleigh number R_o will the kinetic energy increase.

Since R is assumed to be a given quantity whereas R_o varies with the wave number α, the maximizing of the left hand side quantity in equation (5.6a) is the same as minimizing the critical Rayleigh number R_o. Therefore the two selection rules are roughly equivalent to each other.

To show that equation (5.6a) is the same as the criterion obtained before, we rearrange the terms and obtain

$$R = \overline{\gamma}_1 \overline{\gamma}_1' \left(1 + \frac{1}{\alpha^2}\right) + \frac{T}{\alpha^2} \frac{\overline{\gamma}_1'}{\overline{\gamma}_1} \quad (5.6b)$$

which is the same as equation (4.2) (for k = 1, $\lambda = 0$ and $\overline{\gamma} = \overline{\gamma}_1 = \overline{\gamma}_2$) and reduces to equation (5.2) when $q \to 0$, $\overline{\gamma}_1 = \overline{\gamma}_1' = (1 + \alpha^2)$.

It may be mentioned that our consideration of the selection of a most preferred scale only implies that this component has the largest amplitude and therefore represents a distinct entity.

6. CONVECTION IN SATURATED CONDITIONALLY UNSTABLE AIR

Since the tropical atmosphere is only conditionally unstable, we shall investigate the effects of the stable descending motion on the character of the perturbations and on the stability criterion in this section. To simplify the analysis, we take S as a positive constant (S_1) in the ascending region ($0 < r < r_1$) and a negative constant ($S = S_2 = -\ell^2 S_1$) in the descending

region ($r > r_1$). The vertical function P(z) is assumed to be given by $P(z) = \sin \pi z/h$, therefore the problem is reduced to the finding of the horizontal function $\phi(r)$.

It may be remarked that even though the stability criterion and the most preferred scale of motion depend upon viscosity, the general character of the perturbations in such a fluid can be obtained from the nonviscous solution, which is much simpler than the viscous solution. We shall therefore discuss the nonviscous solution first.

A. Nonviscous solution

The nonviscous solution for the case with a stable descending region and q = 0 has been discussed by Haque [6] and by Lilly [10]. The two most important results obtained by these authors are: (i) the vertical velocity w has a finite discontinuity across the surface which separates the ascending from the descending region, and (ii) the ratio of the area of the ascending motion to that of the descending motion decreases as the ratio $\ell^2 = -S_2/S_1$ increases. These conclusions hold also when the viscous effect is taken into consideration. Because of the importance of these conclusions, we shall redevelop the nonviscous solution briefly and obtain some additional information.

The functions $\phi(r)$ which satisfies (4.1a) in the two regions are

$$\phi_1 = A\, \xi\, J_1(\alpha \xi), \qquad o < r < r_1 \tag{6.1a}$$

$$\phi_2 = B\, \xi \left\{ H_1^1(i\beta\xi) + C\, H_1^2(i\beta\xi) \right\}, \qquad r > r_1 \tag{6.1b}$$

where $\xi = \frac{\pi r}{h}$, J_1 is the first order Bessel function, H_1^1 and H_1^2 are the two first order Hankel functions, and α, β, B, and C are given by

$$\left.\begin{aligned} &\alpha^2 = \frac{f^2 + q^2}{g'S_1 - q^2}, \qquad \beta = \alpha/\ell', \qquad \ell'^2 = \frac{g'S_1\ell^2 + q^2}{g'S_1 - q^2}. \\ &B\left\{H_1^1(i\beta\xi_1) + C\, H_1^2(i\beta\xi_1)\right\} = AJ_1(\alpha\xi_1), \quad C = -H_1^1(i\beta\xi_2)/H_1^2(i\beta\xi_2). \end{aligned}\right\} \tag{6.1c}$$

We note that α, β, and ℓ' depend on q^2. When q^2 is close to its limiting value $g'S_1$, both α and ℓ' become infinite while β remains finite. When ξ_2 is large, C approaches zero and ϕ_2 is represented by the first term alone.

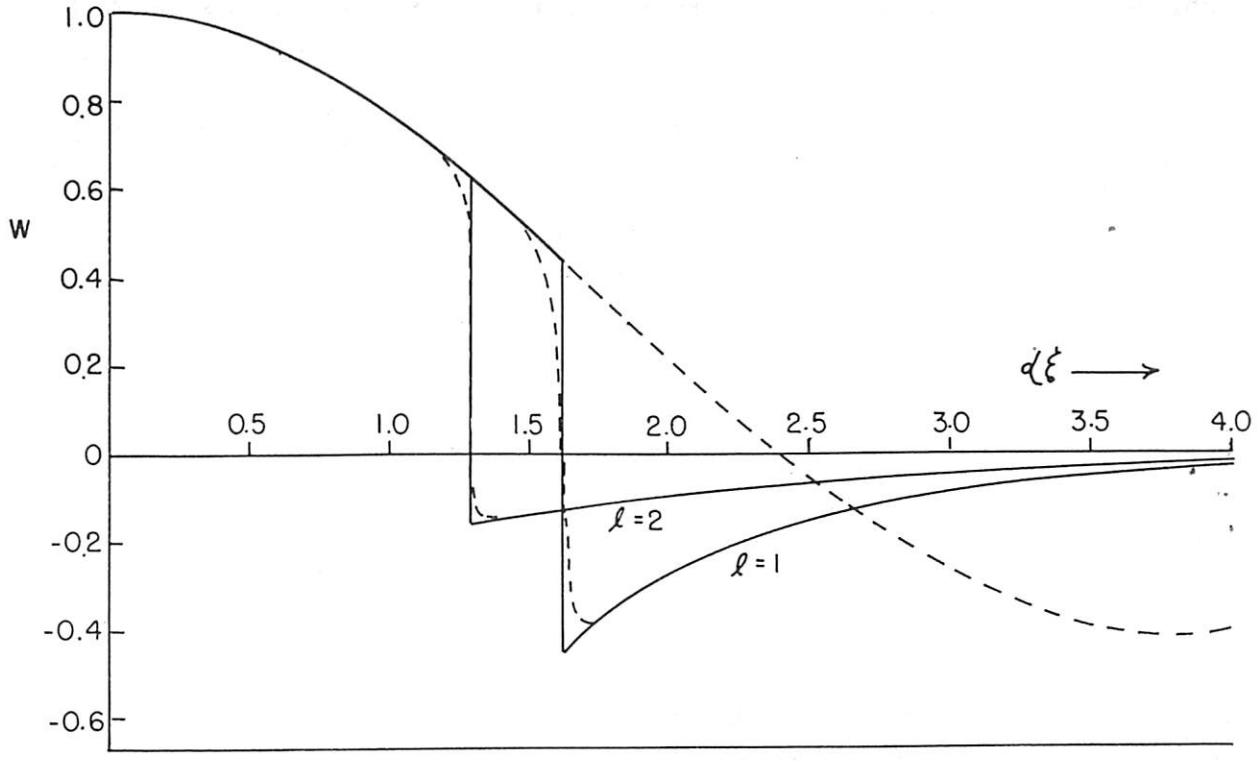

Figure 5. - Variation of w with ξ for $\ell = 1$ and $\ell = 2$ in conditionally unstable atmosphere. Solid curves given by inviscid solution. Dashed curves given by viscous solution.

The variation of the horizontal functions of w in the two regions are represented in figure 5 for the two cases with $\ell' = 1$ and $\ell' = 2$. It is seen that the larger is ℓ', the smaller is the value of $|w_2|$ at $\xi = \xi_2$, and the slower is the variation of w_2 with increasing ξ. That is to say, the more stable are the surroundings, the more widespread is the descending motion.

The ratio of the area of the ascending region to that of the descending motion can be obtained from the compatibility equation, which is obtained by the substitution of the solutions (6.1a,b) into the boundary condition (3.3). For relatively large values of $\beta\xi_1$ and $\beta\xi_2$ this equation is given by

$$\tanh\beta(\xi_2 - \xi_1) = -\ell' \frac{i H_o^1(i\beta\xi_1)}{H_1^1(i\beta\xi_1)} \frac{J_o(\alpha\xi_1)}{J_1(\alpha\xi_1)} \qquad (6.2)$$

which is obtained by making use of the asymptotic approximations of the Hankel functions.

Equation (6.2) has an infinite number of roots, the first one of which is interesting to us. The values of this root corresponding to different values of ℓ' and of $\beta(\xi_2 - \xi_1)$ are given in table 2. It is seen that for a given

Table 2. - Values of $\alpha \xi_1$ as given by (6.2) for different values of $\beta(\xi_2 - \xi_1)$ and ℓ'.

$\beta(\xi_2 - \xi_1) \backslash \ell'$	1	2	3	5	10
∞	1.615	1.28	1.12	0.97	0.83
2.5	1.605	1.27	1.11	0.96	0.83
2.0	1.59	1.26	1.10	0.95	0.82
1.5	1.57	1.25	1.09	0.94	0.81
1.0	1.45	1.10	0.96	0.84	0.71
0.5	1.10	0.82	0.72	0.65	0.54

ℓ', $\alpha \xi_1$ decreases with decreasing $\beta(\xi_2 - \xi_1)$, showing that the placing of a fixed wall at a finite distance reduces the area of the ascending motion. This conclusion is similar to that reached by Bjerknes [1], and has been obtained by Lilly. However, this effect is prominent only when $\beta(\xi_2 - \xi_1)$ is smaller than 1.5. For still larger values of $\beta(\xi_2 - \xi_1)$, $\alpha \xi_1$ is almost equal to its optimum value corresponding to $\xi_2 = \infty$.

According to (6.1c) the factor ℓ' attains its minimum value when $q = 0$, and attains its maximum value when q has its maximum. Therefore the largest possible ascending area for given values of ℓ and ξ_2 is that of the steady state solution, which we shall call the "limiting" motion, while the smallest ascending area is that of the fast growing disturbance. Taking $f = 5 \times 10^{-5}$ sec.$^{-1}$ (20 deg. lat.), $gS_1 = 5 \times 10^{-5}$ sec.$^{-2}$, h = 5 km., we find $\alpha_o = 0.707 \times 10^{-2}$ for the "limiting" disturbance. For this value of α, the values of the maximum radius r_m of the ascending region for different values of ℓ and $\xi_2 = \infty$ are given in table 3. It is seen that these values of r_m are of the same order of magnitude as that of the rain areas of the tropical storms. These values suggest that somehow they represent the most favored scale of motion, although the results obtained from the linearized equations for conditionally unstable saturated air tend to select a much smaller scale of convection. In the last section we shall discuss a semi-nonlinear process which favors these maximum values r_m.

B. Viscous solution and stability criterion

The amplification rate q of the other disturbances can be obtained by joining the two solutions (6.1a,b) at $\xi = \xi_1$, and making use of the relation (6.2). The manipulation is complicated and will not be carried out here.

Table 3. - Radius of ascending region of the limiting disturbance for different values of ℓ, h = 5 km., $\alpha = 0.007$

ℓ	1	2	3	5	10
$\alpha \xi_1$	1.615	1.28	1.12	0.97	0.83
r_m (km.)	362	288	252	218	187

Instead we shall determine the critical value of R and favored scale of motion for marginal instability from the viscous solution by application of the energy integral.

When viscosity is included, the function ϕ for marginal stability is the solution of the equation

$$(D^2 - 1)^3\phi - R\, D^2\phi - T\,\phi = 0, \qquad D^2 = \xi \frac{d}{d\xi} \frac{1}{\xi} \frac{d}{d\xi} . \tag{6.3}$$

and is given by

$$\phi = \sum_{s=1}^{3} A_s \xi\, Z_1(\alpha_s \xi) \tag{6.4}$$

where α_s are the roots of equation (5.2) and Z_1 stands for the Bessel functions in the ascending region and the Hankel functions in the descending region (where $R_2 = -\ell^2 R_1$). It can be seen from equation (5.2) that for large R_1 and large T, the three roots are given by

$$\alpha_1^2 \simeq T/R_1, \qquad \alpha_2^2 = -\sqrt{R_1}, \qquad \alpha_3^2 = +\sqrt{R_1} . \tag{6.4a}$$

Since α_3 is real and its magnitude is much larger than α_1 when R_1 is large, A_3/A_1 must be very small in order to have w remain positive for $\xi < \xi_1$. Therefore the solution in the ascending region is given by

$$\phi_1 = A\,\xi \left\{ J_1(\alpha_1 \xi) + \frac{\alpha_1}{R_1^{1/4}} \frac{J_o(\alpha \xi_1)}{J_o(i\, R_1^{1/4} \xi_1)}\, i\, J_1(i\, R_1^{1/4} \xi) \right\}. \tag{6.4b}$$

It may be mentioned that the hydrostatic approximation cannot be used in this region when friction is included. On the other hand, this approximation may be assumed as valid for the descending region. We then have

$$\phi_2 = B\,\xi \left\{ H_1^1(i\beta_1\xi) - \frac{\beta_1}{\beta_2}\,\frac{H_o^1(i\beta_1\xi_1)}{H_o^1(i\beta_2\xi_1)}\,H_1^1(i\beta_2\xi) \right\},$$

$$\beta_1^2 = T/\ell'^2 R_1, \qquad \beta_2^2 = \ell'^2 R_1. \tag{6.4c}$$

The variation of w with ξ as given by these solutions are represented by the dashed curves for $\ell' = 1$ and $\ell' = 2$ in figure 5. It is seen that the viscous terms of these solutions contribute very little except very close to $\xi = \xi_1$. We shall therefore neglect these viscous terms and take (6.1a,b) as the solution in applying the energy integral. We shall also neglect the variation of ρ_o in these solutions. Putting

$$u = -A\cos\frac{\pi z}{h}\,\frac{\phi}{\xi}, \qquad w = A\sin\frac{\pi z}{h}\,\frac{1}{\xi}\,\frac{d\phi}{d\xi} \tag{6.5a}$$

where ϕ is given by (6.1a,b), we find that θ' and v are given by

$$\left.\begin{aligned}
\theta_1' &= -\frac{1}{\kappa}\,\frac{\partial\theta_{o1}}{\partial z}\,\frac{h^2}{\pi^2}\sin\frac{\pi z}{h}\,\frac{A\alpha}{1+\alpha^2}\,J_o(\alpha\xi) + \dots \\
\theta_2' &= -\frac{1}{\kappa}\,\frac{\partial\theta_{o2}}{\partial z}\,\frac{h^2}{\pi^2}\sin\frac{\pi z}{h}\,\frac{A\beta i}{1-\beta^2}\,\frac{J_1(\alpha\xi_1)}{H_1^1(i\beta\xi_1)}\,H_o^1(i\beta\xi) + \dots \\
v_1 &= \frac{A\,T^{1/2}}{1+\alpha^2}\cos\frac{\pi z}{h}\,J_1(\alpha\xi) + \dots \\
v_2 &= \frac{A\,T^{1/2}}{1-\beta^2}\cos\frac{\pi z}{h}\,\frac{J_1(\alpha\xi_1)}{H_1^1(i\beta\xi_1)}\,H_1^1(i\beta\xi) + \dots
\end{aligned}\right\} \tag{6.5b}$$

where α stands for α_1 and β stands for β_1, and the dots represent the viscous term of the solutions which is to be neglected in the energy integral, (5.4a). Substituting these functions into equation (5.4a), setting $\partial K/\partial t$ to zero, and making use of the relation $\ell\beta = \alpha$, we obtain

$$R\left(1 - \frac{1+\alpha^2}{1-\beta^2}\,I_1\right) = (1+\alpha^2)^2 + \frac{1}{\alpha^2}\left[T + (1+\alpha^2)^2\right] I_2 \tag{6.6}$$

$$I_1 = \frac{1 + (H_o/H_1)^2}{1 + (J_o/J_1)^2}, \qquad I_2 = \frac{\left(\frac{J_1}{H_1}\right)^2 H_o H_2 - J_o J_2}{J_o^2 + J_1^2}. \tag{6.6a}$$

Table 4. - Values of I_1 and I_2 for various values of ℓ

ℓ	1	2	3	5	10
I_1	0.24	0.25	0.23	0.21	0.17
I_2	0.76	0.75	0.77	0.79	0.83

where J_o and J_1 are Bessel functions of argument $\alpha\xi_1$ and H are Hankel functions of the first kind, of orders zero, one, and two and argument $i\beta\xi_1$. Since β is usually very small, we may neglect β^2 against 1 in the left hand side of equation (6.6).

The values of I_1 and I_2 for various values of ℓ are given in table 4. It is seen that they are almost constant. We shall take $I_1 = 0.20$ and $I_2 = 0.80$ for all values of ℓ. Equation (6.6) then becomes

$$(1 - 0.2\chi)\, R = \chi^2 + \frac{0.8}{\chi - 1}(T + \chi^2) \tag{6.7}$$

where $\chi = 1 + \alpha^2$.

As a function of χ, R attains its minimum value when χ is given by

$$(4.8 - 1.6\chi)(T + \chi^2) = 2\chi(\chi - 1)(5.2\chi - 1 - \chi^2) + \chi^2(\chi - 1)^2. \tag{6.8}$$

For sufficiently large T, the equations (6.7) and (6.8) lead to the following asymptotic expressions for the most favored wave number α_m and the lowest critical Rayleigh number R_m:

$$\alpha_m \to \sqrt{2}\,, \qquad R_m \to T \tag{6.9}$$

These asymptotic relations reveal a fundamental difference between the present case of conditional instability and that of absolute instability discussed in the preceding sections. Here, for sufficiently large T, the critical value of R is equal to T, therefore the critical potential temperature gradient is given by

$$gS_m = \frac{K}{\nu} f^2. \tag{6.9a}$$

Thus the value of S_m is determined by f^2 and the Prandtl number, and it is independent of the actual values of the coefficients of viscosity and conductivity.

The other result is that α_m approaches a constant limit $\sqrt{2}$ for large T instead of increasing with T indefinitely, showing that in a conditionally

Table 5. - Values of α_m and R_m for different values of T

T	0	10	100	1000
α_m	0.625	0.975	1.27	1.39
R_m	8.25	25.2	125.	1003.

unstable fluid layer, further increase of rotation beyond a certain value does not have the effect of reducing the horizontal dimension of the ascending motion.

The roots of equation (6.8) have been computed for various values of T and are given in table 5 in terms of α_m, together with the corresponding values of R_m. It is seen that these α_m values are smaller than those in table 1 and the R_m values are higher. This latter effect is to be expected because the stratification is stable in the descending region. It is also seen that for $T > 10^3$, α_m and R_m are very accurately given by the asymptotic relations (6.9).

It may be mentioned that for convection in a conditionally unstable atmosphere, the descending motion can be considered as occurring in the whole space for every perturbation except the area of the ascending motion of this perturbation, therefore the scale of the motion is defined for the ascending motion only.

7. SOLUTIONS FOR VERTICALLY VARIABLE S

In natural convection, the unstable layer is usually not bounded by solid surfaces but by more stable layers, and the mean lapse rate usually varies with height. To examine the effects of these factors, we shall consider three different cases: (a) An unstable layer bounded by a solid surface below and by a stable layer above. (b) An unstable layer sandwiched between two stable layers. S is assumed to be constant in each layer for these two cases. (c) An unstable layer bounded by a solid surface below, with S decreasing linearly with height and becoming stable in upper levels. This last model is more realistic and therefore shall be studied more thoroughly, while the cases (a) and (b) will be discussed only very briefly.

In obtaining the solutions corresponding to a vertically variable S, it will be assumed that the horizontal variation is represented by a harmonic function $F(x,y)$ satisfying (4.1a). For simplicity, the operator $\mathcal{L}$ shall be replaced by a constant multiple γ as given in (4.3). Then the vertical function $P(z)$ is determined by the following equation

$$\frac{d^2P}{d\zeta^2} + \frac{gS - \gamma^2}{f^2 + \gamma^2}\alpha^2 P = 0 \qquad (7.1)$$

where $\zeta = \pi z/h$, h being the depth of the unstable layer.

Case a. $S = S_1 > 0$ for $z < h$

$S = S_2 = -\ell^2 S_1$ for $h < z < \infty$.

The solutions of equation (7.1) in the two layers are

$$P_1 = A_1 \sin k_1 \zeta, \qquad P_2 = A_2 e^{-k_2 \zeta}$$

$$k_1^2 = \frac{gS_1 - \gamma^2}{f^2 + \gamma^2}\alpha^2, \qquad k_2^2 = \frac{gS_1\ell^2 + \gamma^2}{f^2 + \gamma^2}\alpha^2. \tag{7.2}$$

Substitution of these solutions in the condtions (3.4) yields

$$\frac{k_1}{k_2} = -\tan(k_1\pi). \tag{7.2a}$$

This equation has been discussed in some detail by Lilly [10].

The function P as given by (7.2), with k_1 and k_2 satisfying (7.2a), is represented in figure 6 for different values of ℓ. These curves show that the more stable the upper layer is (larger ℓ), the faster will the disturbance be damped out in the stable layer, and the nearer is the level of maximum P moved toward the middle of the unstable layer.

Case b. For this case it is convenient to shift the origin to the middle of the unstable layer. We then have

$S = S_1 > 0$ for $|z| < h/2$

$S = S_2 = -\ell^2 S_1$ for $|z| > h/2$

Assuming the depths of the stable layers are infinite, we then have

$$P_1 = A_1 \cos k_1 \zeta, \qquad P_{2,3} = A_2 e^{\mp k_2 \zeta}. \tag{7.3}$$

Applying the internal boundary conditions (3.4) we obtain

$$\frac{k_2}{k_1} = \tan\left(\frac{k_1\pi}{2}\right). \tag{7.3a}$$

In studying the stability problem when the unstable layer is bounded by stable layers it is convenient to introduce an effective depth (H) of the unstable layer. For the present case, it may be defined as twice the distance between the maximum point $\zeta = 0$ and the point $k_1 \zeta = \pi/2$. For case a, H may be defined as twice the value of z where P has its maximum. These definitions

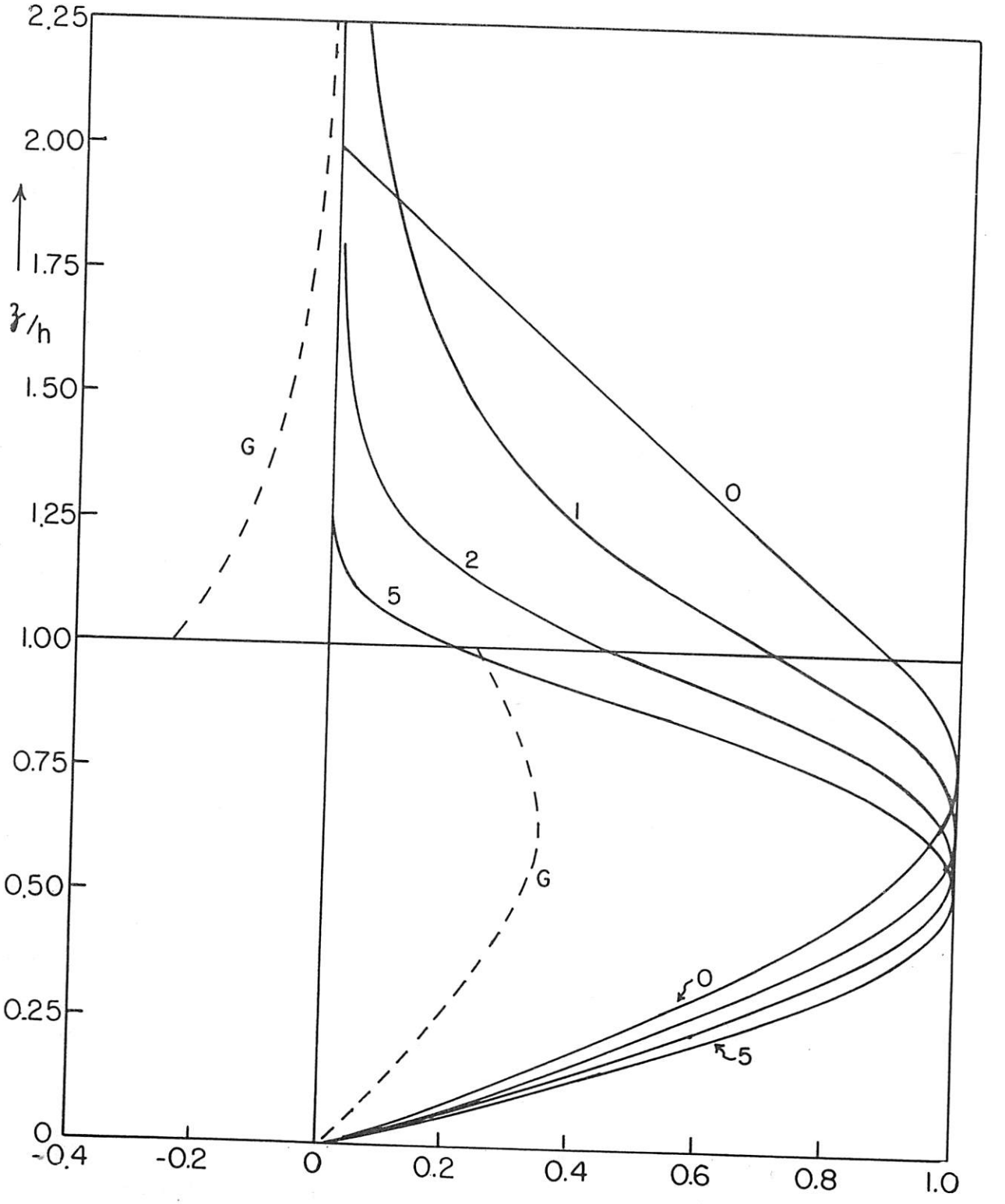

Figure 6. - Variations of the vertical function P with height as given by the two-layer constant S model. The numbers attached to the P-curves are the values of ℓ. Dashed curve G represents temperature perturbation.

Table 6. - Values of the effective relative depth H/h.

ℓ	1	2	3	5	10
Case a	1.334	1.174	1.102	1.066	1.033
Case b	2.00	1.420	1.256	1.144	1.068

give $H = \pi h/k_1$. The values of H/h for these two cases and for different values of ℓ are given in table 6. It is seen that H is always greater than h, but approaches h when the bounding layers are extremely stable.

The perturbation potential temperature θ' is given by

$$\theta' = - \frac{h^2}{\gamma_z \pi^2 (k^2 + \alpha^2)} \frac{\partial \theta_o}{\partial z} \, w \tag{7.4}$$

Since w is continuous but $\partial\theta_o/\partial z$ is discontinuous for these two cases, θ' has a finite discontinuity across the internal boundaries and changes its sign there, as is represented by curve G in figure 6. This is a definite defect of these discontinuous models.

Case c. S decreases linearly with height and the unstable layer is bounded below by a fixed plane, so that the distribution of S is given by

$$S = B \, (1 - z/h) \tag{7.5}$$

where $B = B_1$ for $z < h$ and $B = B_2 = \ell^2 B_1$ for $z > h$, and both B_1 and B_2 are positive.

For this vertical distribution of S, the equation for P can be simplified by the transformation

$$A\xi = \pi \left(\frac{z}{h} - 1 + \frac{\gamma^2}{B} \right) \cong \pi \left(\frac{z}{h} - 1 \right) \tag{7.6a}$$

$$A = \left(\frac{f^2 + \gamma^2}{B\alpha^2} \pi \right)^{1/3}. \tag{7.6b}$$

It may be mentioned that if the hydrostatic approximation were used, the last term on the right side of (7.6a) would be absent. In this case, the zero point of ξ is at $z = h$ and it is positive in the stable layer and negative in the unstable layer. We shall refer to this approximation in the illustrations.

Substituting this transformation into equation (7.1) reduces it to

$$\frac{d^2 P}{d\xi^2} - \xi P = 0. \tag{7.7}$$

The solutions of this equation can be expressed in terms of the Hankel functions of order 1/3 and argument $\xi^{1/2} / 3^{1/3}$; or more conveniently, in terms of the Airy integrals Ai(ξ) and Bi(ξ):

$$P(\xi) = C_1 \text{ Ai } (\xi) + C_2 \text{ Bi } (\xi). \tag{7.8}$$

The functions Ai (ξ) and Bi (ξ) are oscillatory for negative ξ (i.e., in the unstable layer), with their amplitude decreasing as ($-\xi$) increases. For positive ξ (i.e., in the stable layer), Ai (ξ) decreases and Bi(ξ) increases exponentially with increasing ξ (see H. Jeffreys [7], and British Association of Mathematical Tables [2]).

When the stable layer extends to infinity, we must exclude Bi (ξ) from P_2. Therefore P_2 is given by

$$P_2 (\xi) = C_1^1 \text{ Ai } (\xi'). \tag{7.8a}$$

where ξ' is defined by (7.6a) with $B = B_2$ in A, while P_1 is given by (7.8). Substituting these two solutions into the two conditions (3.4) we find

$$\begin{aligned} C_1 &= \frac{C_1^1}{2} \left\{ 1 + \left(\frac{B_2}{B_1} \right)^{1/3} \right\} \\ C_2 &= \frac{C_1^1}{3.4641} \left\{ 1 - \left(\frac{B_2}{B_1} \right)^{1/3} \right\}. \end{aligned} \tag{7.9}$$

When $B_1 = B_2$, we have $C_1 = C_1^1$, $C_2 = 0$, and $\xi' = \xi$. Therefore the solution is represented by (7.8a) at all levels. We shall discuss this case only.

The lower boundary is at $\xi = \xi_1$. At this boundary we must have

$$\text{Ai } (\xi_1) = 0. \tag{7.10}$$

The first root of this equation is $\xi_1 = -2.3381$, giving A = 1.3436. From the relations (7.6a,b) we then find

$$\frac{f^2 + \gamma^2}{B\alpha^2} \pi = 2.4258 \left(1 - \frac{\gamma^2}{B}\right)^3. \tag{7.11}$$

This equation determines the amplification rate q as a function of the horizontal wave number α and the stability parameter B.

Neglecting the higher powers of γ^2/B on the right side of this equation we then find γ is given by

$$\gamma^2 = \frac{0.772 \alpha^2 B - f^2}{1 + 2.31 \alpha^2}. \tag{7.12}$$

Table 7. - Values of α_m and R_{oc} for different values of T.

T	0	5	10	100	1000
α_m	0.61	0.89	1.00	1.56	2.37
R_{oc}	12.2	23.1	30.1	94.9	372.0

This is to be compared with equation (4.2).

From equation (7.11) we find the critical Rayleigh number is given by

$$R_o = 3\,(1 + \alpha^2)^2 + \frac{1.295}{\alpha^2}\left\{T + (1 + \alpha^2)^2\right\} \qquad (7.13)$$

where $R_o = gB_1 h^4 / K\nu\pi^4$, which is equal to twice of the mean R of the unstable layer.

For a given T, R_o attains its minimum when α is given by

$$\alpha^6 + 1.2158\,\alpha^4 = 0.2158\,(T + 1). \qquad (7.14a)$$

The values of α_m given by this equation and the corresponding R_{oc} are given in table 7. It is seen that these values of α_m and $R_{oc}/2$ are smaller than those in table 1.

For sufficiently large T, α_m, and R_{oc} are given by

$$\alpha_m \to 0.7725\,T^{1/3}$$

$$R_{oc} \to 3.23\,T^{2/3} \qquad (7.14b)$$

which are of the same form as (5.3a), but with different numerical coefficients.

The variation of P as a function of z for this case ($B = B_1$) is represented by the full curve in figure 7. The maximum value of P occurs at $z = 0.5641\,h$, which is lower than that of case a for $\ell = 1$.

When the stable layer is of finite depth h', we must include Bi (ξ) in the solution. However, when h' is not too small compared with the depth h of the unstable layer, the result differs very little from that for an infinite h', as is indicated by the dashed curve in figure 7, which represents the P-function for $h' = h$.

The vertical variation of the perturbation potential temperature θ' in the ascending region is represented by the curve G in figure 7. It is seen that for this case θ' changes its sign continuously across the boundary at $z = h$. In this respect the continuous model is much better than the

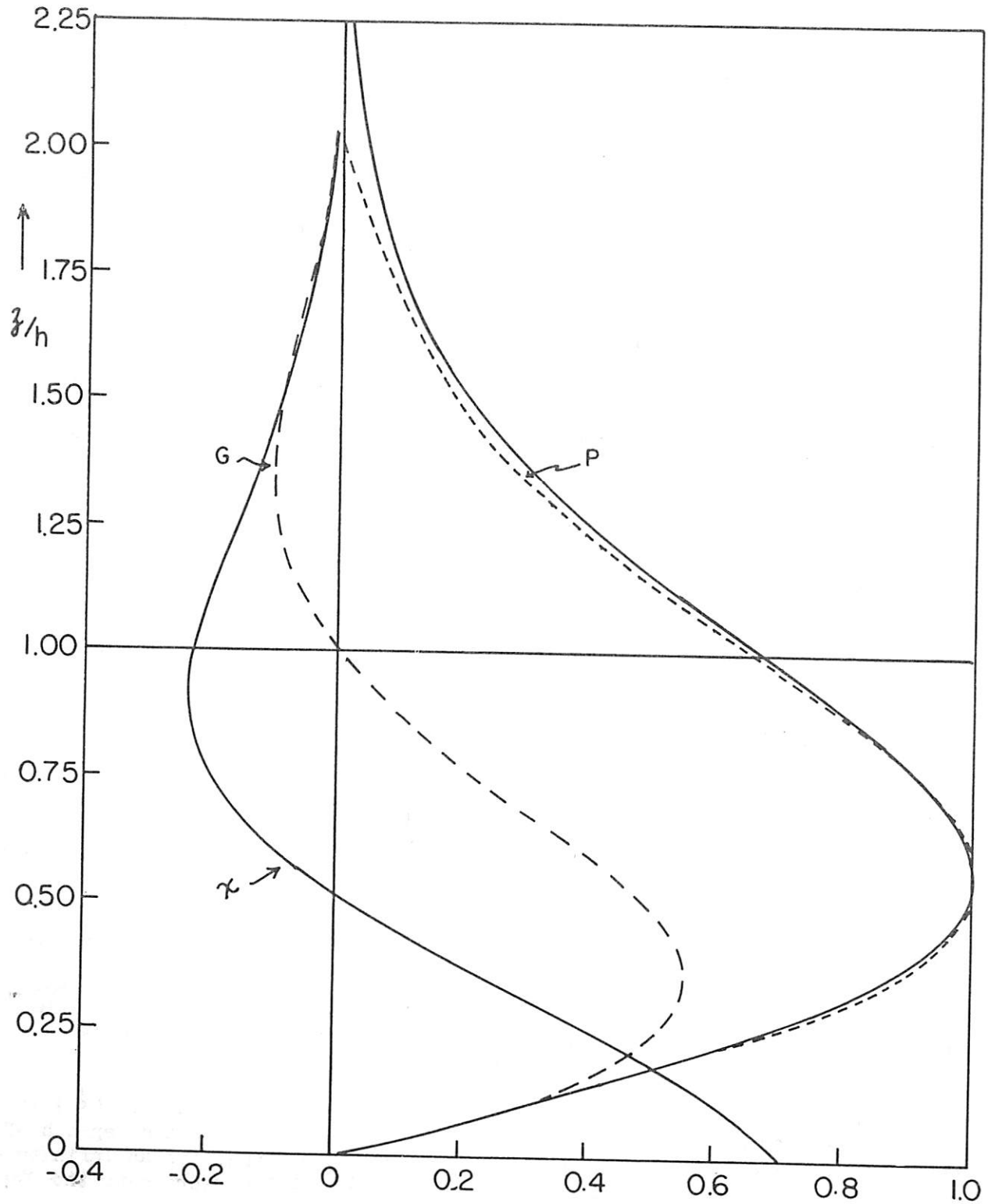

Figure 7. - Vertical variation of P, G (temperature), and χ (tangential momentum) functions when S increases linearly with height.

discontinuous model, even though they give similar vertical distributions of velocity and pressure.

From the equations (2.10 - 2.13) we find that the vertical variation of $\rho_o v$ is given by the function χ, and the vertical variations of $\rho_o u$ and P' are given by $-\chi$, where χ is defined by

$$\chi = \frac{\partial}{\partial z} (P e^{-\sigma z/2}). \tag{7.15}$$

This function has also been plotted in figure 7. It is seen that low pressure and cyclonic circulation occupy the lower part of the unstable layer while in the upper levels the pressure is high and the circulation is anticyclonic.

These solutions show that the most important effects of the vertical variation of S are the diminution of the perturbation intensity in the stable layer and the shifting of the level of maximum vertical motion from the top toward the middle of the unstable layer. The more stable the upper layer is, the faster will the disturbance be damped out in this layer, and the nearer is the level of maximum P to the middle of the unstable layer.

8. VERTICAL TRANSPORT OF HEAT AND MODIFICATION OF MEAN TEMPERATURE DISTRIBUTION BY CONVECTION

In this section we shall determine the vertical transport of heat and the modification of the mean temperature distribution by convection and calculate the maximum velocity attainable from the realization of the unstable stratification. The calculations will be based on the solutions for the parabolic θ_o-profile obtained in the preceding section, case c, which can be taken as a good approximation to the real atmospheric condition.

A parabolic θ_o-profile may be visualized as being maintained by radiation and evaporation in the atmosphere, with the ground and the ozone layer as the two main immediate sources of heat, which absorb solar radiation directly. We shall approximate the radiation process by the combination of an equivalent conduction (Brunt [3] and Goody [5]) and a distribution of cold sources in the atmosphere, which takes away the heat that is conducted into the atmosphere from the heat sources.

For convenience, we introduce h, h^2/K, and $\nu K \bar{\theta}_o/gh^3$ as the units of length, time, and temperature, respectively, and convert the equations into nondimensional forms. The eddy conductivity K and the eddy viscosity coefficient ν are both assumed to be constant. We also write $R = \frac{gh^4}{K\nu\bar{\theta}} \frac{\partial\bar{\theta}}{\partial z}$ as the Rayleigh number.

Combining the thermodynamic equation and the continuity equation, and integrating over the entire horizontal plane in question and assuming that there is no net transport of heat across the boundary we obtain the following equation for the mean potential temperature

$$\frac{\partial \bar{\theta}}{\partial t} + \frac{1}{\rho_o} \frac{\partial(\rho_o \overline{w\,\theta'})}{\partial z} = \frac{\partial^2 \bar{\theta}}{\partial z^2} + Q \tag{8.1}$$

Q being the internal cold source. The variation of ρ_o in the second term is not important and will be disregarded from the present consideration.

We shall consider the equilibrium steady states for $\bar{\theta}$. The variation of temperature before convection sets in, which we denote by θ_o, is governed by the two terms on the right side of equation (8.1). It is evident that to maintain a parabolic θ_o-profile in steady state, it is necessary to have a uniform cold source Q_o ($= -R_o$) to remove the inflow of heat.[2]

Subtraction of the equation for θ_o from equation (8.1) results in the following equation for $\tilde{\theta}$ ($\equiv \bar{\theta} - \theta_o$)

$$\frac{\partial^2 \tilde{\theta}}{\partial z^2} = \frac{\partial(\overline{w\,\theta'})}{\partial z} - Q_1 \tag{8.2}$$

where $Q_1 = Q - Q_o$ is the additional heat source needed to maintain a steady state when there is convection, which will be determined below. Integrating this equation once and again, we obtain.

$$\frac{\partial \tilde{\theta}}{\partial z} = \beta_o + \overline{w\,\theta'} - Q_1 z \tag{8.3a}$$

$$\tilde{\theta} = \tilde{\theta}_o + \beta_o z + \int_o^z \overline{w\,\theta'}\, dz - \frac{1}{2} Q_1 z^2 \tag{8.3b}$$

where β_o denotes the value of $\frac{\partial \tilde{\theta}}{\partial z}$ at $z = 0$, and $\tilde{\theta}_o$ is the value of $\tilde{\theta}$ at $z = 0$.

In order to fix the constants β_o, $\tilde{\theta}_o$ and Q_1 we must make use of the boundary conditions. Since the disturbance decreases exponentially with height in the stable layer and is already very small at $z = 2$, we may assume that $\tilde{\theta}$ is to vanish at this height and above, even when the depth of the stable layer is infinite.

Using the condition $\tilde{\theta} = 0$ at $z = 2$ in equation (8.3b) it gives

---

[2] If the cooling is proportional to the temperature, the steady state θ_o-profile will be sinusoidal. The solution of the seminonviscous equations will then be represented by Mathieu functions in z. The basic character is the same as that for the parabolic profile discussed here.

$$Q_1 - \beta_o - \frac{1}{2}\tilde{\theta}_o = \frac{1}{2}\int_o^{z_1} \overline{w\,\theta'}\, dz, \qquad z_1 \geq 2. \tag{8.3c}$$

Additional conditions are needed in order to determine the three constants. Since convection and conduction only redistribute the heat, we shall assume the following requirements

$$\text{(i)}\ \ \tilde{\theta}_o = 0, \qquad \text{(ii)}\ \ \int_o^{z_1} \tilde{\theta}\, dz = 0, \qquad z_1 \geq 2. \tag{8.4a}$$

Integrating (8.3b) once again and making use of (8.4a) we obtain

$$\frac{2}{3} Q_1 - \beta_o = \frac{1}{2}\int_o^2 \int_o^z (\overline{w\,\theta'})(dz)^2. \tag{8.5}$$

Since $\tilde{\theta}_o$ is assumed to be zero, the two equations (8.3c) and (8.5) determine Q_1 and β_o in terms of the integrals of $\overline{w\,\theta'}$.

For the parabolic θ_o-profile we may use the solution obtained in section 7. The solution w and θ^1 are given by

$$w = C_1\, Ai(\xi)\ \ F(x,y) \tag{8.6a}$$

$$\theta' = \frac{C_1 \pi^2}{(k^2+\alpha^2)}\, R_{oc}\, (1 - z)\, Ai(\xi)\, F(x,y) \tag{8.6b}$$[3]

where F (x,y) is the horizontal harmonic function, C_1 is an arbitrary constant, and R_{oc} is the critical value of R_o. It should be mentioned that since these are the solutions of the linearized equations, we must use R_{oc} in (8.6b).

From these solutions we find $\overline{w\,\theta'}$ is given by

$$\overline{w\,\theta'} = \frac{C_1^2 \pi^2 R_{oc}}{2(k^2+\alpha^2)}\ \ (1 - z)\, Ai^2(\xi). \tag{8.7}$$

---

[3] Here, as in (6.5), we are using the approximation that the application of the Laplacian operator in the viscous terms is equivalent to a multiplication by $-(k^2 + \alpha^2)$.

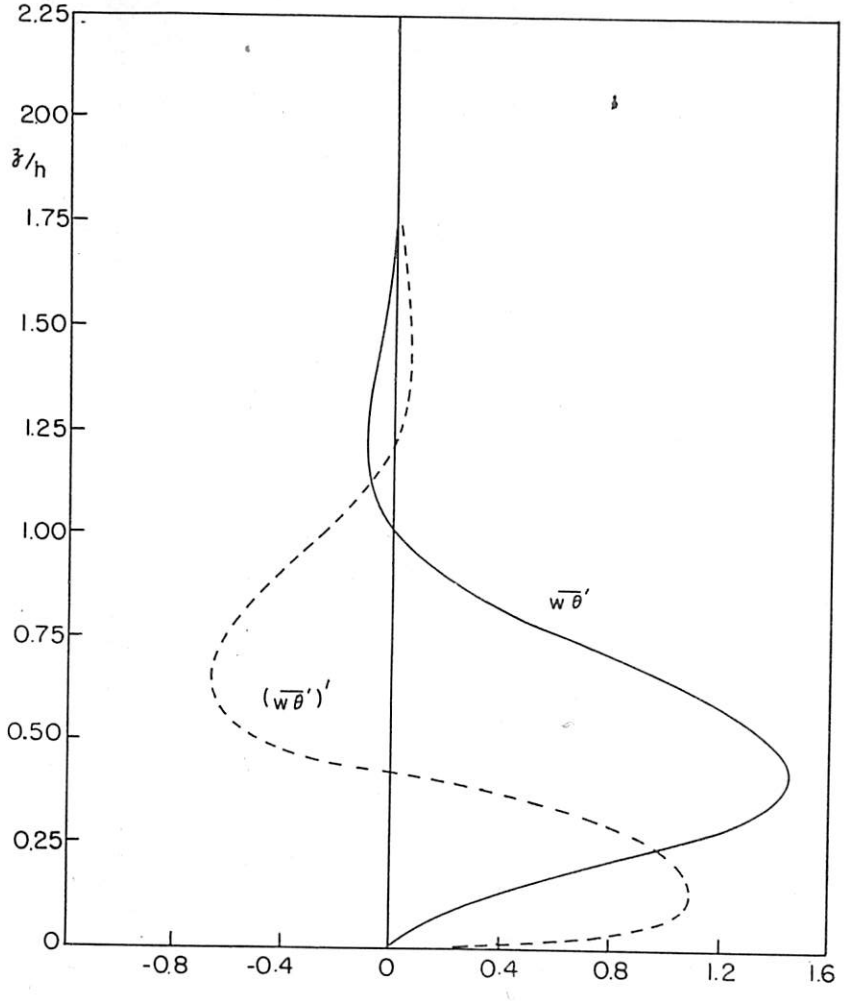

Figure 8. - Vertical variation of the convective heat transport $\overline{w\,\theta'}$ and its derivative.

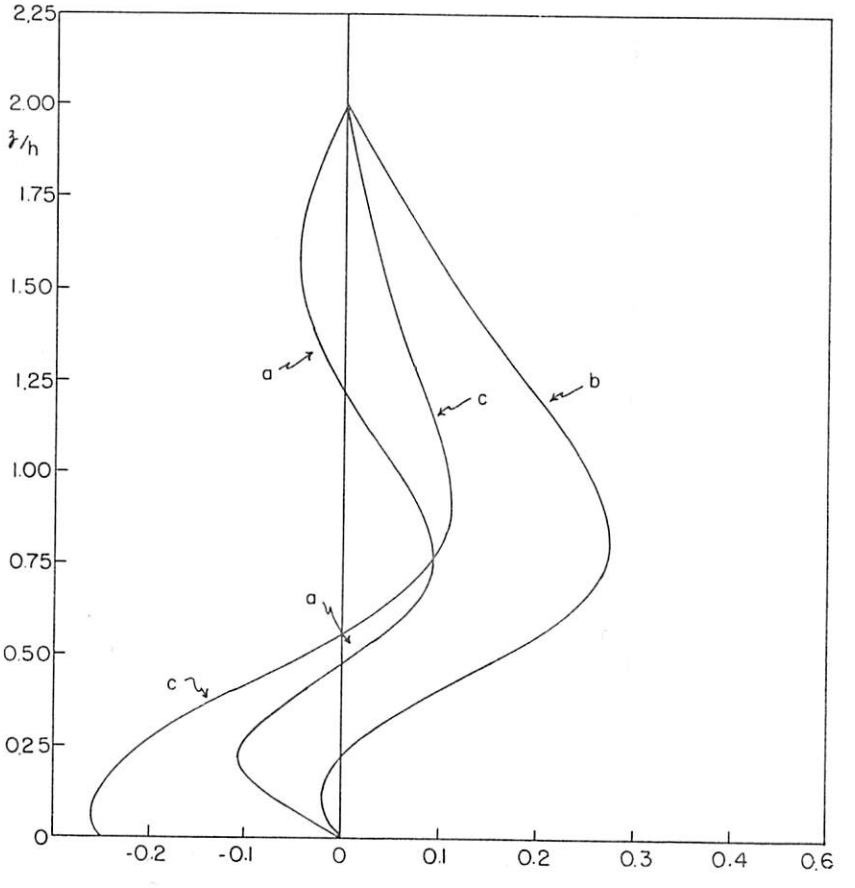

Figure 9. - Modification of mean temperature distribution by convection. Curve a for condition (8.4a). Curves b and c correspond to conditions (8.4b,c).

The variation of this function and its derivative are represented in figure 8. It is seen that there is a divergence of the convective heat flux in the lower part of the unstable layer and in the upper part of the stable layer and a convergence in the middle.

Substituting (8.7) into (8.3c) and (8.5), solving for Q_1 and β_o and then substituting into (8.3b) we finally obtain

$$\tilde{\theta} = \frac{AK}{\pi} \left\{ H(\xi) + 0.07695\, z^2 - 0.23627\, z \right\}.$$

$$H(\xi) = \frac{\pi}{A} \int_0^z (1 - z)\, Ai^2(\xi)\, dz, \quad A = 1.3436, \quad K = \frac{C_1^2 \pi^2 R_{oc}}{2(k^2 + \alpha^2)}. \tag{8.8}$$

The variation of this $\tilde{\theta}$ with z is represented in figure 9 by the curve a, the units being $\Delta R = R_o - R_{oc}$, i.e., the excess of R_o over its critical value. Note that this $\tilde{\theta}$ is quite similar to $-\partial(\overline{w\,\theta'})/\partial z$ given in figure 8. It reduces the value of $\partial\bar{\theta}/\partial z$ in the lowest layer and also in the upper part of the unstable layer and lower part of the stable layer, and augments $\partial\bar{\theta}/\partial z$ in the middle part of the unstable layer. Thus as a result of convection, the mean temperature gradient is closer to the adiabatic lapse rate except it becomes more stable near the top and more unstable near the bottom, and the level where $\partial\bar{\theta}/\partial z$ changes sign has been raised.

The curves b and c in figure 9 represent the solution which satisfy the requirements

$$\tilde{\theta}_o = 0 \quad \text{and} \quad Q_1 = 0, \quad \text{but} \quad \int_0^2 \tilde{\theta}\, dz \neq 0. \tag{8.4b}$$

$$Q_1 = 0 \quad \text{and} \quad \int_0^2 \tilde{\theta}\, dz = 0, \quad \text{but} \quad \tilde{\theta}_o \neq 0. \tag{8.4c}$$

It appears that these two conditions are not as realistic as condition (8.4a).

The as yet unspecified constant C_1 can be determined by substituting the solutions into the thermal energy integral which we shall derive immediately. The essence of this method which was first introduced by Stuart [11] in studying other fluid motion problems, is to take the solution of the linearized equations as the first approximation of the nonlinear solution, and to utilize an appropriate energy integral to determine the intensity.

Multiplying the thermal energy equation by θ' and integrating over the entire volume, assuming that there is no net transport across the boundaries, we obtain

$$\overline{\frac{\partial \bar{\theta}'^2}{\partial t}} - \overline{\bar{R}\,\overline{w\theta}'} = \overline{\theta' \nabla^2 \theta'} \tag{8.12a}$$

$$\begin{aligned} \bar{R} &\equiv -\frac{\partial \bar{\theta}}{\partial z} = -\frac{\partial \theta_o}{\partial z} - \frac{\partial \tilde{\theta}}{\partial z} \\ &= R_o (1 - z) - \frac{\partial \tilde{\theta}}{\partial z} = R\pi^4 \end{aligned} \tag{8.12b}$$

where R stands for the actual Rayleigh number, when convection is present, and the bar denotes an average over the horizontal plane and the bracket denotes an average over the vertical. Substituting this R into equation (8.12a) and assuming that a steady state has been established for the convection it gives

$$\int_o^\infty \left\{ \overline{w\theta'} R_o (1 - z) + \overline{\theta' \nabla^2 \theta'} \right\} dz = \int_o^\infty \overline{w\theta'} \frac{\partial \tilde{\theta}}{\partial z} dz. \tag{8.13}$$

We mention that because the solutions are based on the critical value R_{oc}, the left hand side of this equation differs from zero when $R_o > R_{oc}$. Furthermore, since the left side contains C_1^2 while the right side contains C_1^4, this equation determines C_1^2.

Substituting $\overline{w\theta'}$ from (8.7), $\frac{\partial \tilde{\theta}}{\partial z}$ from (8.3a) and θ' from (8.4b) we find

$$C_1^2 = \pi^2 (k^2 + \alpha^2) \frac{I_1}{I_2} \eta^2 \tag{8.14}$$

where $\eta^2 \equiv \frac{R_o}{R_{oc}} - 1$ and I_1 stands for the difference of the thermal energy released from the undisturbed temperature distribution and the dissipation of temperature variance by conduction, and I_2 is proportional to the energy stored up in $\tilde{\theta}$ which is given by the integral

$$\int_o^\infty \overline{w\theta'} \frac{\partial \tilde{\theta}}{\partial z} dz.$$

For the three different sets of boundary condtions (8.4a, b, c) discussed above, we find the following three values for the ratio I_1/I_2:

(a) 15.15, (b) 25.06, (c) 11.45. (8.15)

These results show that more thermal energy has been converted into kinetic energy when the boundary temperature is fixed and the volume mean temperature is allowed to increase, and less kinetic energy is created if

the bottom temperature is allowed to fall. However, the difference is not very significant.

As an example, let us take $f = 5 \times 10^{-5}$ sec.$^{-1}$, h = 5 km. (depth of unstable layer), $\nu = \kappa = 70$ m.^{2} sec.$^{-1}$, giving T = 3. From (7.14a) and (7.13) we find $\alpha_m = 0.82$, $R_{oc} = 19.6$. For a surface stability factor $S_o = 2.5 \times 10^{-5}$ m.$^{-1}$, we find $R_o = 3.1 \times 10^5$, giving $\eta^2 = 1.55 \times 10^4$. Using this value of η^2 in (8.14) and putting in the dimensional factor κ/h in w we find the maximum vertical velocity attainable with conditions (8.4a) is 14.7 m.sec.$^{-1}$, while that with the conditions (8.4b) is 19 m. sec.$^{-1}$. The horizontal velocities u and v attainable by these convective motions are about 25 m.sec.$^{-1}$. The change of the mean temperature is a cooling of about 4°C. in the middle troposphere. If, however, the cumulus cloud scale convection is suppressed by some physical processes such as the entrainment of the dry air, then the large scale perturbations will have a chance to grow. The kinetic energy will then be mainly in the horizontal motions.

9. COMPOSITE VARIATION

Since the mean atmosphere is conditionally unstable in the lower layer, we must obtain the solution for the case when S is negative both in upper levels and in the descending region. Aside from the application of these solutions to the present problem of convection in a conditionally unstable atmosphere, they also illustrate the property of the solutions when the differential equation is hyperbolic in one region and elliptic in another. For simplicity we take $S = S_2 = -\ell^2 S_1$ in all the stable regions. In case of circular symmetry, four different solutions need to be used for the following four regions:

(i) Low level unstable ascending region, $0 < r < r_1$, $0 < z < h$.

$$\Psi_1 = A_1 \sin k_1 \zeta \cdot \xi J_1(\alpha \xi), \quad \zeta = \pi z/h, \quad \xi = \pi r/h. \tag{9.1}$$

(ii) Low level stable descending region, $r > r_1$, $0 < z < h$.

$$\Psi_2 = A_1 \sin k_1 \zeta \, \xi H_1^1(i\beta\xi) \cdot \frac{J_1(\alpha \xi_1)}{H_1^1(i\beta\xi_1)}. \tag{9.2}$$

(iii) High level stable ascending region, $0 < r < r_1$, $z > h$.

$$\Psi_3 = A_1 \sin k_1 \pi \cdot e^{-k_2(\zeta-\pi)} \xi J_1(\alpha \xi) \tag{9.3}$$

(iv) High level stable descending region, $r > r_1$, $z > h$.

The functions (9.1 - .3) are the solutions discussed in sections 6 and 7. In order that the conditions (3.3ii) and (3.4ii) are satisfied, α and β must be related by (6.2) and k_1 and k_2 be related by equation (7.2a).

In region (iv), continuity of Ψ requires Ψ_4 to vary as $e^{-k_2(\zeta-\pi)}$ along the vertical wall ($r = r_1$, $z > h$) and to vary as $\xi H_1^1(i\beta\xi)$ along the horizontal plane ($z = h$, $r > r_1$). However, the product of these two functions is not a solution of the differential equation for region iv, therefore Ψ_4 must be obtained separately.

To simplify the equation for Ψ_4, we introduce the independent variables ζ and η, defined by

$$\zeta = \pi z/h, \qquad \eta = \frac{\pi r}{h}\left(\frac{f^2 + q^2}{g\ell^2 S_1 + q^2}\right)^{1/2}. \tag{9.4}$$

Neglecting friction, the differential equation for Ψ_4 then becomes

$$\eta \frac{\partial}{\partial \eta}\frac{1}{\eta}\frac{\partial \Psi_4}{\partial \eta} + \frac{\partial^2 \Psi_4}{\partial \zeta^2} = 0. \tag{9.5}$$

The solution of this equation that satisfies the boundary conditions $\Psi_4 = 0$ at $\eta = \infty$, $\zeta = \infty$, is found to be given by

$$\frac{\pi}{2}\Psi_4(\eta, \zeta) = \int_0^\infty e^{-k\zeta} \sin k\eta\, dk \left(\int_0^\infty \Psi_{\zeta=0} \sin k\eta_0 d\eta_0\right) + \int_0^\infty e^{-k\eta} \sin k\zeta\, dk \left(\int_0^\infty \Psi_{\eta=0} \sin k\zeta_0 d\zeta_0\right) \tag{9.6}$$

where $\Psi_{\zeta=0}$ and $\Psi_{\eta=0}$ are the values of Ψ_2 and Ψ_3 on the two lines $z = h$ and $r = r_1$, respectively.

10. DISTURBANCES IN UNSATURATED ATMOSPHERE AND INITIATION OF LARGE-SCALE CIRCULATION

The results obtained in the preceding sections show that in a saturated conditionally unstable atmosphere of infinite horizontal extent, all disturbances with a horizontal scale smaller than that of the "limiting perturbation" defined by $\alpha^2 = f^2/gS_1$ can gain kinetic energy from the unstable stratification, but the one with the dimension of a cumulus cloud has the maximum rate

of amplification. If random perturbations of small amplitudes are introduced in such an atmosphere, the cumulus cloud scale convection will grow to the largest amplitude and there seems to be no reason to expect the "limiting perturbation" to become the dominating one. Therefore the existence of the much larger and very distinctive disturbances such as the tropical depressions remains unexplained.

On examining the mean tropical atmosphere as represented by figure 1, we notice that it is actually not saturated and therefore is stable for all infinitesimal perturbations. On the other hand, the latent energy of conditional instability can be realized by finite amplitude perturbations whose vertical velocity is above a certain threshold value, so as to provide enough lift of the air mass and produce saturation. For the tropical atmosphere represented in figure 1, a lift of about 600 meters is needed.

Assuming finite amplitude disturbances of different wavelengths are present in the atmosphere before saturation, we shall now discuss a selection of the scale of motion among these finite amplitude perturbations, first by studying their ability to produce saturation and then by investigating their subsequent development.

Since the atmosphere under consideration is stable before saturation, these perturbations are likely to be oscillatory, with their period-wavelength relationship similar to that of the pure gravitational waves, that is, the longer the wavelength, the longer the period. For the present qualitative discussion of the mechanism we are visualizing, it suffices to take the period-wavelength relation of the gravitational waves as an example, and apply it also to other types of disturbances, including the easterly waves.

We assume that before saturation the motion is represented either by standing waves or waves traveling in the x-direction, so that

$$w = \sum_{\alpha} A_{\alpha} e^{-b_{\alpha} t} \sin \alpha (x + c_{\alpha} t) \sin \frac{\pi z}{h} \tag{10.1}$$

which satisfies equation (2.21) provided the damping factor b_{α} and the phase speed c_{α} satisfy the following relations

$$b_{\alpha} = \frac{\nu_z \pi^2}{h^2} (1 + \alpha'^2), \qquad c_{\alpha}^2 \equiv \frac{\mu_{\alpha}^2}{\alpha^2} = \frac{gs\alpha^2 + f^2}{\alpha^2(1 + \alpha'^2)}. \tag{10.1a}$$

The vertical displacement ζ_{α} produced by the single wave α is then given by

$$\zeta_{\alpha} = \frac{A_{\alpha} e^{-b_{\alpha} t}}{\mu_{\alpha}^2 + b_{\alpha}^2} \left\{ \mu_{\alpha} (1 - \cos \mu_{\alpha} t) - b_{\alpha} \sin \mu_{\alpha} t \right\} \sin \frac{\pi z}{h} \cos \alpha x. \tag{10.2}$$

Taking $gs = 1.4 \times 10^{-4}$ sec.$^{-2}$, $f = 5 \times 10^{-5}$ sec.$^{-1}$, we find the period $P = 10$ min. for $\alpha = 2$ (cumulus cloud scale), $P = 18$ hours for $\alpha = 0.007$

(the limiting perturbation) and P = 35 hours for $\alpha = 0$. Taking the maximum vertical velocity as 3 cm. $sec.^{-1}$ or less, it is evident that only the waves longer than the limiting size can provide the required lift to produce saturation. Therefore the small-scale perturbations are insignificant during the pre-saturation stage of the motion.

Remembering that perturbations larger than the limiting scale will be damped out by friction even in the saturated conditionally unstable atmosphere, it becomes clear that the maximum scale of the growing disturbances is the limiting perturbation defined by $\alpha^2 = f^2/gS_1$. Therefore it is only necessary to analyze the subsequent development of the perturbations whose scale is smaller than the limiting scale.

The most important distinction between the present system and convection in a saturated conditionally unstable atmosphere of infinite horizontal dimension is that in the present system saturation exists only in the ascending region of the larger perturbation, while outside this region the air is unsaturated and more stable. Under this circumstance the upward motions of the smaller disturbances must take place inside this ascending region in order to gain energy from the instability, whereas the descending motions can take place outside. In this way the descending and ascending branches of the small-scale convections are detached from each other and they can contribute directly to the large-scale circulation. On the other hand, in the case of saturated conditionally unstable atmosphere of infinite horizontal extent, ascending motion of the small-scale perturbations can take place anywhere and there is no preference to organize them into a larger circulation.

Although suggestions of the possibility of an organization of small-scale convection cells into large-scale circulation have occasionally been made by synoptic meteorologists and by theoreticians, the kinematics and dynamics of such a process have never been discussed before. A more detailed analysis of this process will be presented in another paper.

11. CONCLUSIONS

If justifications of the various approximations are the closeness of the results they yield as compared with the results obtained from the more exact relations, then the analysis in section 4 shows that the hydrostatic approximation is valid for disturbances whose horizontal scales are much larger than the vertical scale, whereas the balance approximation is valid for the perturbations with smaller horizontal dimensions. In light of this rule and the results obtained in sections 4 and 5, we conclude that in an atmosphere which is statically unstable, whether absolutely or only conditionally (i.e., unstable for ascending motion only), the convective motion that will evolve from random small perturbations will have the dimension of a cumulus cloud. A distinct large-scale circulation can not be created by merely introducing random infinitesimal perturbations in such a situation; some organizing mechanism which has the effect of arresting the enormous growth of the cumulus convection is needed.

On the other hand, if the balance approximation for the circular - or line-symmetric flow is justifiable for the large-scale perturbations from other considerations, then the use of the balance condition and inclusion of the frictional effect in the vertical equation of motion will lead to the development of a large-scale circulation.

The effects of the stable descending motion have been studied in section 6. It has been found that a much larger lapse rate in the ascending region is required to sustain the motion. For a sufficiently large Taylor number T, this critical lapse rate is given by $gS_1 = \frac{K}{\nu} f^2$, while the corresponding most preferred scale is given by $\alpha^2 = 2$. These two results are completely different from that for convection in an absolutely unstable rotating fluid. Another effect of the stable descending motion is that it makes the ascending motion concentrated in a much smaller region and the descending motion widespread, a result obtained in previous studies.

The effect of the stable stratification in upper layers has been analyzed in section 7 through the use of three models, two are composed of unstable and stable layers of constant S, while in the third model S decreases linearly with height. The overall vertical distributions of velocity and pressure obtained from these models are quite similar, both showing a rapid decrease of the perturbation in the stable layer. However, the temperature perturbation obtained from the third model is continuous, showing the desirability of using a continuous model.

The modification of the vertical distribution of the mean potential temperature by convection has been determined in section 8, based on the solution for the continuous parabolic θ_o - profile. It is shown that convection makes the middle troposphere nearly adiabatic (moist) and the upper part more stable. The maximum vertical velocity attainable from the tropical atmosphere is about 15 to 20 m. sec.$^{-1}$, assuming unstable stratification for both ascending and descending motions, while the horizontal velocity may reach 30 m. sec.$^{-1}$, if we assume $\alpha = 2$ for the most preferred motion. For large-scale motion, the motion would be mainly horizontal.

The solutions when S varies both vertically and horizontally are discussed in section 9. It is shown that in the upper and outer part where descending motion is taking place in the absolutely stable air, a composite solution is required.

In section 10 an organizing mechanism is proposed, by taking into consideration the fact that the mean tropical atmosphere is not saturated and therefore is stable for all infinitesimal perturbations. The latent instability can become realized only after saturation has been produced, which we assume to be accomplished by the vertical motion of the perturbation. It is found that a threshold vertical velocity of the order of 2 to 3 cm. sec.$^{-1}$ is needed, and it must be associated with the large-scale perturbations such as the easterly waves in order to be effective. After saturation has been produced in a limited region, it is possible to have the small-scale convection contribute to this large-scale motion.

Other processes that tend to enhance the development of the large-scale circulation are those physical processes which impede the continued growth of the cumulus cloud scale convection, such as the entrainment of dry air and cooling by the falling rain. It seems that a more detailed knowledge of the smaller systems is needed in order to have a complete understanding of the development of the large-scale systems such as tropical storms and hurricanes.

REFERENCES

1. J. Bjerknes, "Saturated-Adiabatic ascent of air through dry-adiabatically descending environment," Quarterly Journal of the Royal Meteorological Society, vol. 64, 1938, pp. 325-330.
2. British Association Mathematical Tables, Volume B, "The Airy Integrals," Cambridge University Press, London, 1946.
3. D. Brunt, Physical and Dynamical Meteorology, Cambridge University Press, London, 1944.
4. S. Chandrasekhar, "The Instability of a Layer of Fluid Heated Below and Subject to Coriolis Forces," Proceedings of the Royal Society, Series A, vol. 217, 1953, pp. 306-327.
5. R. M. Goody, "The Influence of Radiative Transfer on Cellular Convection," Journal of Fluid Mechanics, vol. 1, No. 4, Oct. 1956, pp. 424-435.
6. S. M. A. Haque, "Initiation of Cyclonic Circulation in a Vertically Unstable Stagnant Air Mass," Quarterly Journal of the Royal Meteorological Society, vol. 78, 1952, pp. 394-406.
7. H. Jeffreys and B. S. Jeffreys, Methods of Mathematical Physics, Cambridge University Press, London, 1956.
8. C. L. Jordan, "Mean Soundings for the West Indies Area", Journal of Meteorology, vol. 15, No. 1, Feb. 1958, pp. 91-97.
9. C. L. Jordan, "Mean Soundings for the Gulf of Mexico Area," National Hurricane Research Project Report No. 30, 1959.
10. D. K. Lilly, "On the Theory of Disturbances in a Conditionally Unstable Atmosphere," Monthly Weather Review, vol. 88, No. 1, Jan. 1960, pp.1-17.
11. J. T. Stuart, "On the Nonlinear Mechanics of Hydrodynamic Stability," Journal of Fluid Mechanics, vol. 4, 1958, pp. 1-21.
12. S. Syōno, "On the Formation of Tropical Cyclones," Tellus, vol. 5, No.2, May 1953, pp. 179-185.